A SYSTEM DESIGN OF AN OPTICAL WIRELESS COMMUNICATION SYSTEM FOR CUBESATS

By

SESHUPRIYA REDDY ALLURU

A THESIS PRESENTED TO THE GRADUATE SCHOOL
OF THE UNIVERSITY OF FLORIDA IN PARTIAL FULFILLMENT
OF THE REQUIREMENTS FOR THE DEGREE OF
MASTER OF SCIENCE

UNIVERSITY OF FLORIDA

2010

I dedicate this thesis to my Mum and Aruna akka.

ACKNOWLEDGMENTS

I would like to thank Dr. McNair for consenting to be my advisor and for her constant support, encouragement and guidance through the completion of this thesis. I would like to thank Dr.Ann Gordon Ross and Dr. Fitz Coy for agreeing to be on my supervisory committee.I would like to thank my friends Farida and Prasanthi for being such wonderful and cheerful roommmates.

Finally, I would like to thank my brother and parents.

.

TABLE OF CONTENTS

LIST OF TABLES

LIST OF FIGURES

Abstract of Thesis Presented to the Graduate School
of the University of Florida in Partial Fulfillment of the
Requirements for the Degree of Master of Science

A SYSTEM DESIGN OF AN OPTICAL WIRELESS COMMUNICATION SYSTEM FOR
CUBESATS

By

Seshupriya Reddy Alluru

December 2010

Chair: Janise. Y. McNair
Major: Electrical and Computer Engineering

Optical wireless communications provide a promising, high bandwidth alternative to radio communications, where high performance links are desired. For large satellites (say, wet mass>1000kg), laser cross links have been successfully established since 2001 by various space agencies in Europe and Japan. Thus far, the cross-links have been able to achieve data rates in Gbps range for distances greater than 10,000km. Such gains would be monumental improvement for communications in small satellite domain , where the typical communication payload uses radio antenna that achieve an average data rate of 10kbps. The thesis looks at exploring the components of an Intersatellite Laser Link System for large satellites that is responsible for establishing cross links as a means of communication and the feasibility of a similar system to achieve long distance crosslinks for the CubeSat. A brief study of the laser crosslink system of the large satellites is provided. Then, the parameters and requirements of the subsystems are discussed and determined for the CubeSat frame. An analysis of the contribution to the weight of the CubeSat and power consumption requirements are performed with respect to the CubeSat specifications. A link budget analysis was carried out through simulations for the optical system and it was seen that distances upto 200km were achievable with error free communications.

CHAPTER 1
INTRODUCTION

1.1   Introduction

A CubeSat is a miniaturised satellite (10x10x10 cm, weighing 1 kg) which offers all the standard functions of a normal satellite (attitude determination and control, uplink and downlink telecommunications, power subsystem including a battery and body-mounted solar panels, on-board data handling and storage by a CPU, plus either a technology package or a small sensor or camera). They can even have deployable solar panels, antennas or booms. Limited orbit control using micropropulsion, S-band instead of VHF/UHF and wireless data transfer inside the CubeSat are now beginning to be used. It takes about two years to develop a CubeSat from the provision of funding until launch. The hardware cost of a CubeSat is in the range 100,000 USD. Up to now, about 40 CubeSats have been successfully launched, worldwide an estimated 70-100 CubeSats are being readied for launch in the next few years.

A single CubeSat is simply too small to also carry sensors for significant scientific research. Hence, for the universities the main objective of developing, launching and operating a CubeSat is educational. However, when combining a large number of CubeSats with identical sensors into a network, in addition to the educational value, fundamental scientific questions can be addressed which are inaccessible otherwise. Networks of CubeSats have been under discussion in the CubeSat community for several years, but so far no university, institution or space agency has taken the initiative to set up and coordinate such a powerful network. CubeSat reliability is not a major concern because the network can still fully achieve its mission objectives even if a few CubeSats fail. Such a network of satellites is being built and deployed by the QB50 program involving a list of space agencies such as National Aeronautical Space Agency(NASA), European Space Agency(ESA),(Innovative Solutions in Space) ISIS and universities such as California Polytechnic Sate University. Use of radio frequency

communications for applications that require low data volumes is a convenient and standard approach, while data intensive applications would benefit from the high data rate availability of optical communications. Lasers, with their high directionality and low power requirements, promise to be a better way to implement long distance high data rate space communications. For very long distances, because of a polynomial relationship between power and distance, multi-hop communication is much more power efficient than long range, direct source to sink communication. For example, the greater power efficiency comes from the ability to emit a highly directional beam, radiating very little power in unintended directions. In addition,a typical cube satellite RF antenna has a power rating of 500 mW, while the typical power rating for a laser transmitter used in large satellites is about 100mW. Lasers operate at frequencies much higher than radio microwave frequencies. Hence, they have the potential to provide higher data rates. For example, successful tests have been conducted among large satellites to achieve a free-space optical link operation at speeds of up to 40 Gbps, which is sufficient for high resolution image or video or any other data intensive operations. Also, Long range RF communication links, because of their weak signal strengths, are susceptible to jamming and thus are prone to DOS (Denial of Service) attacks. By using multi-hop communications, much better signal strengths can be achieved, which means more robustness against DOS attacks. Inter-satellite laser communication is the key to power efficiency, security and more importantly for deployment of any distributed system like a CubeSat cluster. In addition, because of their high directionality, laser communications are very robust against jamming and electromagnetic interference.

A preliminary survey of the traditional use of small satellites has shown that inter-satellite communications have not been a high priority. In many cases, the communications intent has been simply to be able to ping the small satellite, to receive short control commands from a ground station, and to transfer very small amounts of

data back to the ground station intermittently. Thus, most configurations use simple antennas for communication. Typical characteristics are summarized in the table 1-1.

Table 1-1. Typical communication characteristics of small satellites

Characteristic	Minimum	Maximum	Typical
Data Rate	1200 bps(e.g, CanX1, Cute1)	38.4kbps(e.g., AeroCube2)	9600bps
Power	350 mW(e.g., Cute-1.7)	2W(e.g., AeroCube)	500mW
Total download	320 KB(e.g, CP4)	6.77 MB(e.g, CSTB1)	0.5-5 MB

1.2   History of Optical Crosslinks

Large satellite laser communications was begun in the early 2000s, with the European Space Agencys effort to launch its Advanced Relay and Technology Mission Satellite (ARTEMIS) (in July 2001) and demonstrate laser communications ability using the SILEX (Semi-Conductor Inter Satellite Link Experiment) optical communications system.

1.2.1   Semi-Conductor Inter-Satellite Link Experiment (SILEX)

Almost thirty years ago, in summer 1977, European Space Agency (ESA) placed a technological research contract for the assessment of modulators for high data-rate laser links in space. This marked the beginning of a long and sustained ESA involvement in space optical communications. Recognizing the potential performance edge of optical communications over RF technologies in terms of size, weight and power, ESA placed during the past two decades a large number of study contracts and preparatory hardware developments, conducted under various ESA R& D and Support Technology Programs. In mid 1980's, ESA took an ambitious step by embarking on the SILEX program, to demonstrate a pre operational optical link in space. The SILEX Phase A and B studies were conducted around 1985, followed by technology bread-boarding and pre development of the main critical elements, which were tested on

the so-called System Test Bed, to verify the feasibility of SILEX. A detailed design phase was carried out in parallel with the System Test Bed activities up to July 1989.

1.2.2 Advanced Relay and Technology Mission Satellite (ARTEMIS) and Optical Ground Station(OGS)

In 1993 developments of a satellite independent laser communication terminal check-out facility began in Tenerife, Spain. The facility, called optical ground station (OGS), became operational by end of 2000. Also in the early 2000s, the ESA experiment with ARTEMIS began. ARTEMIS carries payloads for the demonstration and promotion of advanced technologies and services, in particular data relay, land mobile communications and navigation. The pre-shipment review of ARTEMIS took place in ESA at the end of 1999, and the launch of ARTEMIS was initially scheduled for February 2000 on the Japanese launcher H2A. Problems with the Japanese launcher, however, made it necessary to look for an alternative launch option in order to avoid further delays. Eventually, ARTEMIS was launched on 12 July 2001 on Ariane 5, but (due to under performance of the third stage of the Ariane 510 launcher) the satellite was left in a far too low elliptical orbit (about 17500 km x 590 km instead of 36000 km x 860 km). Within 10 days, and by using most of its on-board propellant for a total of 8 motor firings, ARTEMIS was brought into a circular, however non-geostationary, orbit with 31000 km altitude, a 0.8 degrees inclination and an orbital period of 20 hours. In order to check out as early as possible the health of the SILEX payload on ARTEMIS, first tests with ESAs optical ground station on Tenerife were performed on 15 November 2001 at 01:00 UTC. Pointing, acquisition and tracking of the satellite were demonstrated and two link sessions of 20 minutes each were performed. The OGS/ARTEMIS space to ground link statistics count, 137 sessions of which 25 failed with an accumulated link duration of 2 days, 10 hours and 37 minutes.

Eventually, with help of its ion thrusters initially foreseen for North/South station keeping ARTEMIS was spiralled out to its geostationary (GEO) orbital position of 21.5^o

East. The maneuver lasted from beginning of 2002 until February 1st, 2003 during which no satellite operations were possible, because the thrust direction required a spacecraft attitude change away from nominal Nadir pointing.

1.2.3   ARTEMIS and Satellite Pour l'Observation de la Terre(SPOT)-4

As mentioned above, the SILEX Phase A and B studies were conducted around 1985, with a detailed design phase carried out in parallel with the System Test Bed activities up to July 1989. At that time, SPOT-4, a French space agency (CNES) satellite was being developed, and SILEX phase C/D with an optical terminal was integrated into SPOT-4. This was an important decision, as it made a suitable partner satellite available for the ESA data-relay satellite project. In 1998, SPOT-4 was launched. After the initial launch of ARTEMIS, specifically, in November 2001, SPOT-4 operating at 832km, and ARTEMIS, operating at 31,000km, exchanged the first-ever transmission of an image by laser link from one satellite to another satellite. The linking was performed using SILEX between the Opale terminal on ARTEMIS and the Pastel terminal on the SPOT 4 satellite. The terminals exchanged high-definition imagery data at 50 megabits per second. ARTEMIS subsequently beamed the data at its leisure to the receiving station operated by Spot Image at Toulouse, using a conventional 20 GHz radio link. After ARTEMIS reached its final orbital destination, the SPOT-4/ARTEMIS inter-satellite link statistics since March 2003 count 1327 sessions, of which 57 failed, with an accumulated link duration of 10 days, 18 hours and 30 minutes.

1.2.4   ARTEMIS and Optical Inter-orbit Communication Engineering Test Satellite(OICETS)

The Japanese Space Exploration Agency (JAXA) conducted the first conceptual design and feasibility study of Kirari, also known as the Optical Inter-orbit Communication Engineering Test Satellite (OICETS), in 1992. In 1993 JAXA and ESA agreed on a cooperation to perform optical communication experiments between OICETS and ARTEMIS. The preliminary design of OICETS (and its laser communication terminal

called LUCE) was finished in 1994 and the flight model ready in 2001. JAXA validated the performance of the engineering model of its LUCE terminal in a space to ground link with ARTEMIS from ESAs OGS in September 2003. OICETS was launched on August 23rd, 2005 into a circular sunsynchronous 610 km orbit and the first laser communication experiments with ARTEMIS were performed on December 9th, 2005. Unlike SPOT-4, OICETS can also receive data and it demonstrated the worlds first bidirectional optical inter-satellite communication link. All subsequent links have been successful, with very short acquisition times and excellent tracking performances. These links were constantly being measured for the approximately 15 hours of experiments. The OICETS/ARTEMIS inter-satellite link statistics counts 83 sessions of which 2 failed, with an accumulated link duration of 14 hours and 21 minutes. The DLR Institute for Communication and Navigation performed 8 space-groundlessness communication experiments with OICETS.

1.2.5 ARTEMIS and Liaison Optique Laser Aroporte(LOLA)

LOLA (Liaison Optique Laser Aroporte) was a French national demonstrator program to achieve an optical link between an airborne carrier representative of the future medium- and high-altitude unmanned area vehicle (UAVs) (MALE and HALE) and ARTEMIS. The purpose of the experiment was to characterize the propagation of light beams in the atmosphere and to validate the system performance capabilities of the link. The link was to be used for secure transmission of information received from UAVs by operation centres a few thousand kilometres away, within about one second and at very high data rates. This high capacity data stream could considerably reduce the time need to transmit information from the theatre of operation, would improve control of information and would bring significant operational advantages.

In December 2006, ARTEMIS successfully relayed optical laser links from Mystre 20, equipped with the airborne laser optical link LOLA. At that time, the airborne laser links, established over a distance of 40,000 km during two flights at altitudes of 6000

and 10,000 meters, represented a world first. The relay was set up through six two-way optical links between LOLA on Mystre 20 and the SILEX laser link payload on board ARTEMIS in its geostationary orbital position.

1.2.6   Near Field Infrared Experiment(NFIRE) and TerraSAR

The latest laser communication terminal to be launched is the SOLACOS system, which was developed by the German Space Agency to fly on TerraSAR, a German funded Earth observation satellite using synthetic aperture radar in X-band. Solid State Laser Communications in Space(SOLACOS), manufactured by Tesat Spacecom, Germany, and based on coherent binary phase shift keying modulation at 1064nm, was originally intended as a possible return channel for SILEX, using a data rate of 5.6 Gbps over link distance up to 10,000 km. However, its partner terminal for a laser communication demonstration between LEO satellites was launched on board the American NFIRE satellite. In 2008, NFIRE and TerraSAR demonstrated the fastest in space-borne communications channel to date. Operating in Low Earth Orbit, a 5.5-Gbps inter-satellite bidirectional optical communication link was successfully tested between NFIRE and TerraSAR-X at a range of about 5,000 km.

1.2.7   AlphaSAT

Finally, the AlphaSat spacecraft is a successor to ARTEMIS and is developed in cooperation between ESA and the French Space Agency (CNES). 80% of AlphaSats payload capacity was awarded to Inmarsat Global Ltd to extend the capabilities of its Broad Global Area Network Services which currently consists of a wide range of high date rate applications to a new line of user terminals for aeronautical, land and maritime markets. Figure 1.2.7 gives a representation of the optical crosslinks discussed.

1.2.8   Small Satellite Laser Communications

The state of small satellite laser communications is largely based on laboratory research, with systems being planned. (National Institute of Information and Communication Technology (NICT) is engaged in joint research with Mitsubishi Heavy Industries to
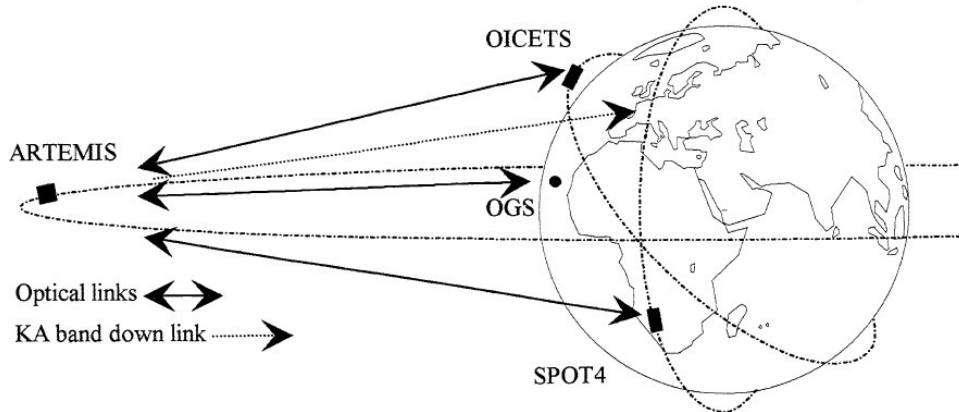
Figure 1-1. SILEX project [5].

launch a small satellite (approx. 150 kg), referred to as SmartSat into an elliptical
orbit for preliminary verification of optical inter-satellite communications. Also at NICT,
the Space Communications Group is developing a non-mechanical, compact optical
terminal equipped with a two-dimensional laser array. The non-mechanical transceiver is
proposed to facilitate a reduction in the size of the optical communications system.

1.3   Mission Scenarios

Small satellites are currently playing an important role in the field of remote sensing.
Optical communications could play an important role in facilitating the development
of data intensive remote sensing applications.[6] gives a detailed survey of the
about the use of the of small satellites in various remote sensing applications. As an
example,Satellites such as the BiSpectral InfraRed Detection (BIRD) experimental
small satellite(2001-2004) have been launched for detection of hot events like forest
fires and volcanic eruptions. Another important application of remote sensing is to
study the effect of environmental change on the patterns of human health and disease.
Use of small satellite imaging can be carried out to study the effects of environmental
parameters that influence spatial and temporal patters of vector borne diseases. A
dedicated remote sensing surveillance system can identify high risk areas wherein
preventive measures can be deployed at the earliest. For malaria, an example relevant

18
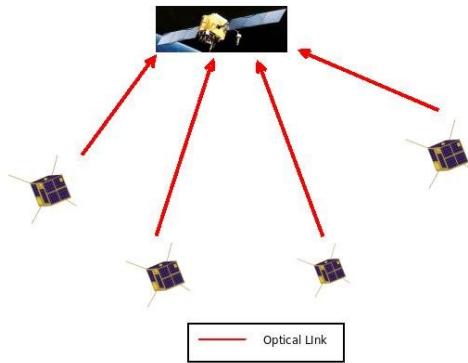
Figure 1-2. Mission scenario

to many other vector-borne diseases, key environmental parameters include the spatial and temporal patterns of vegetation type and condition, land use, standing water, and human settlements. Remote sensing satellites can provide valuable inputs on disaster management both for an accurate prediction and for a rapid assessment of the location and extent of damage. Parameters of remote sensing satellites include spectral coverage, spectral resolution, revisit time and spatial resolution. Current spaceborne infrastructure provides environmental monitoring excellently but not disaster mitigation due to low repetition and bad spatial resolution. An ideal repetition rate of 0.5-1 hour and resolution of 10m-1km is required for disaster mitigation. Clusters of small satellites can solve this problem as the cost to develop and launch several of them is not prohibitive. In order to increase the amount of data transfer a possible mission scenario is show in in figure 1-2 wherein, data collected by the small satellites is transmitted to a larger satellite in the GEO orbit using optical links and the larger satellite transmits the data to the ground station. This scenario not only provides seamless coverage of the area desired and high resolution images but also large amount of data for analysis as the data transfer rates of optical links can go upto several Mbps.

1.4 Intersatelliete Laser Link Components

The Intersatellite laser link system (ISL) of large satellites, includes several components to facilitate the establishment of long distance to deep space crosslinks.

19

However,all the components are not required to achieve the same purpose for crosslinks for CubeSats. The block diagram of the ISL is shown in figure 1.4 for a CubeSat. As stated by [7], a 3U CubeSat can have a maximum weight of 3kgs and the availability of power dependent on the number of solar panels and hence can is assumed to vary from 3-6 Watts. Each of the subsystem will be described in detail with emphasis on the operation, requirements to be met and finally summarizing the parameters for each for the CubeSat.

The thesis is organized in the following manner. Chapter 2 describes the Optical Source and Detector,Chapter 3 the Pointing Acquisition and Tracking System, Chapter 4 the Optical Transmitter and Receiver, Chapter 5 analyses the proposed system, Chapter 6 provides the link budget analysis and comparison with Radio Frequency and Chapter 7 concludes the work.

Optical Transmitter

Optical Source

CPE

From On board processor

PAT System

Electrical Signal

Free Space Channel

Optical Link

Optical Receiver

Optical Detector

CPE

To On board processor

PAT System
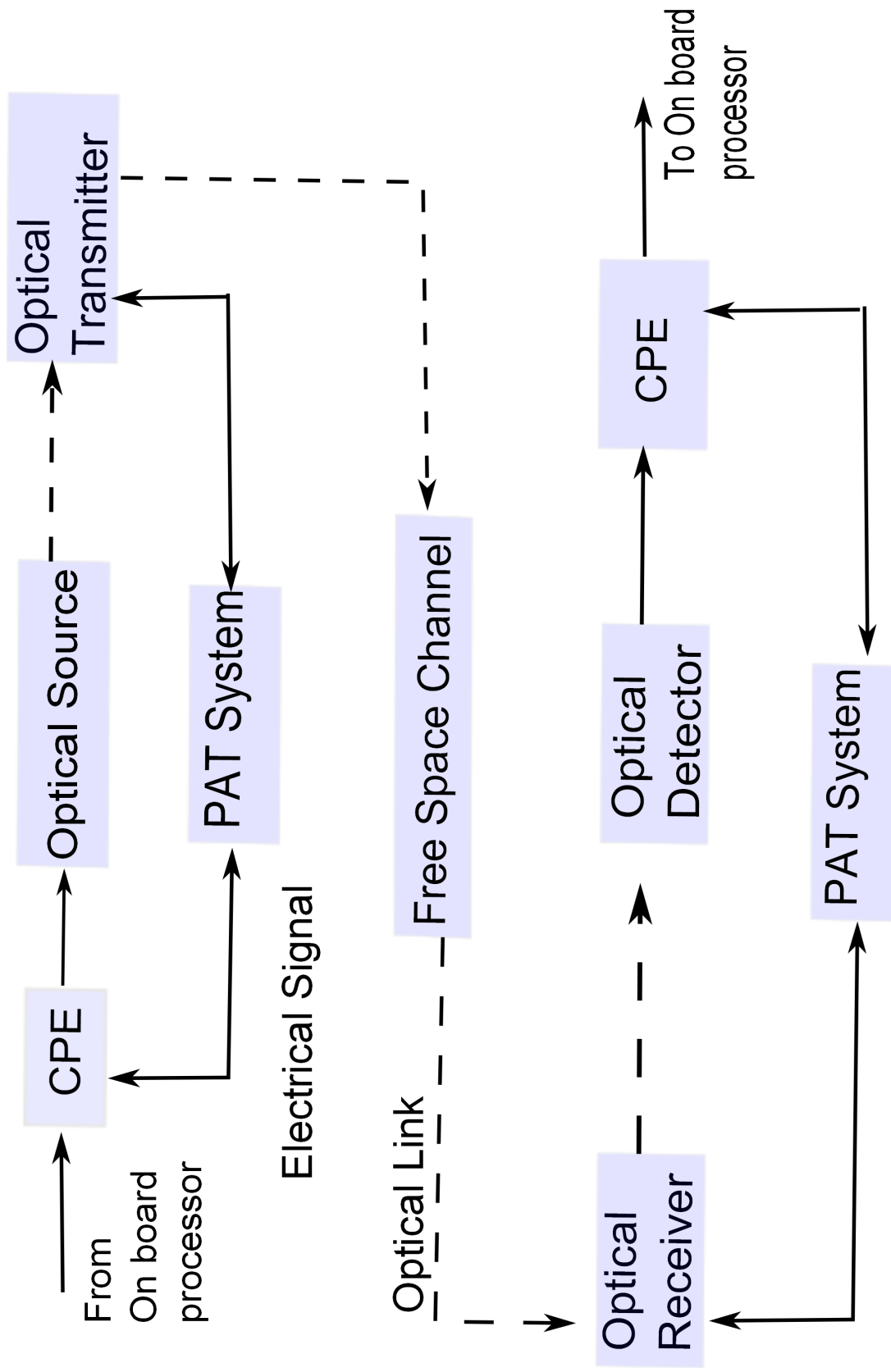
CPE- Communications Processing Electronics   PAT:Pointing, Accquisition & Tracking

Figure 1-3. ISL block diagram

21

Optical
Transmitter

Optical Source

PAT System

CPE

From
On board
processor

Electrical Signal

Free Space Channel

Optical Link

Optical
Receiver

Optical
Detector

PAT System

CPE

To On board
processor
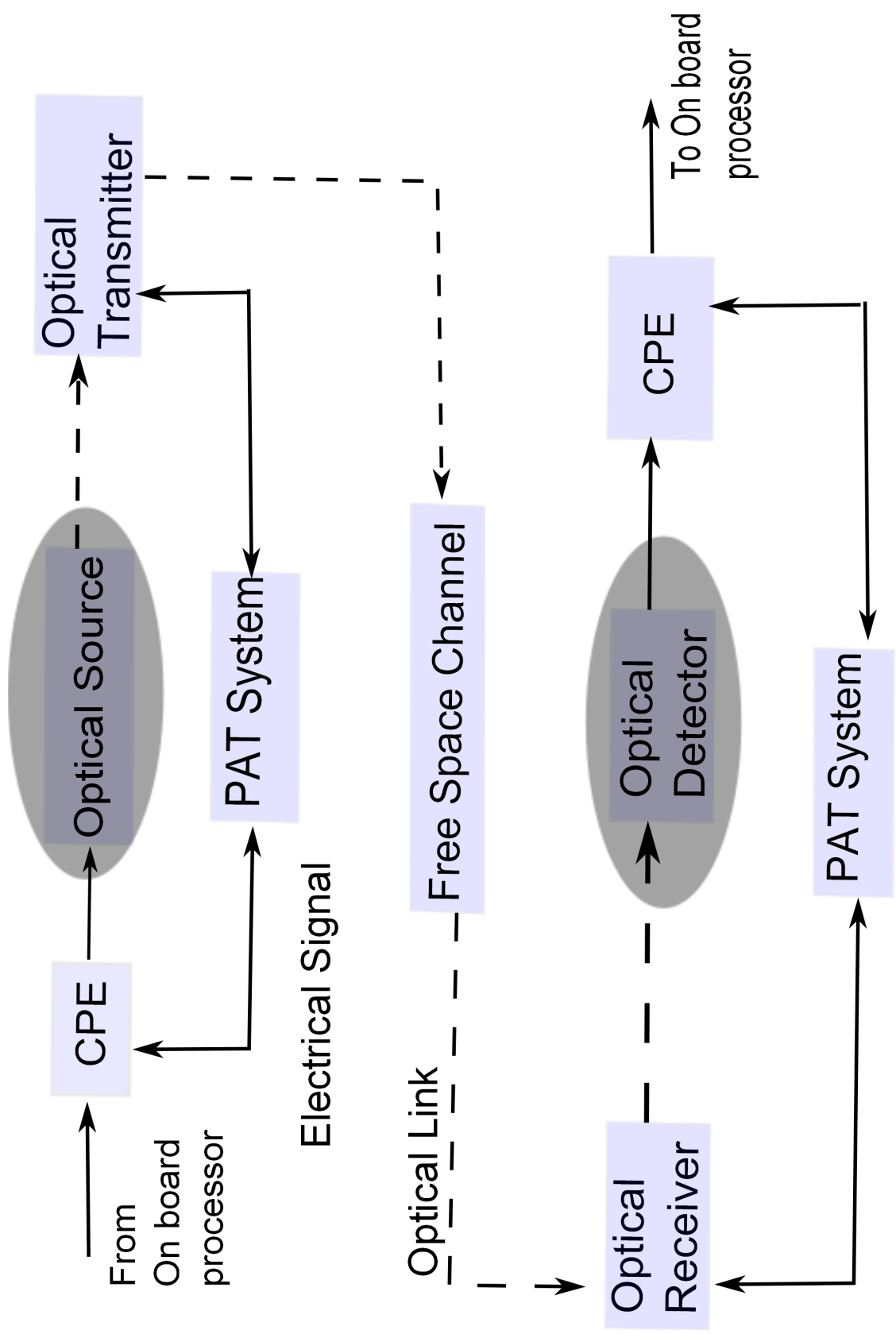
CPE- Communications Processing Electronics   PAT:Pointing, Accquisition &
Tracking

Figure 1-4. ISL block diagram

22

CHAPTER 2
OPTICAL SOURCE AND DETECTOR

The subsystems discussed in this chapter are the optical source and optical detector emphasized in figure 1.4. In the first section the various components and the requirements of the optical source are discussed and the characteristics of the source that can be installed on the CubeSat is summarized. The second section discusses the various optical detectors, their properties and their relevance to the CubeSat.

2.1 Optical Source

The optical source is the device that produces the signal for communication. Such a device that can produce an optical signal is the Laser. Several classification of lasers exist according to the different types of lasing medium that produces the signal. Lasers are classified into Gas, Solid state, Dye and Free electron lasers. Gas lasers are further classified into chemical and excimer lasers. Solid state lasers are further classified into Fibre hosted, photonic crystal and Semiconductor Lasers. In the initial stages of crosslink design, Gas lasers were primarily used as the optical source. Gas lasers require kilowatts of power to be turned at the same time producing a high powered output signal. But their bulkiness and the difficulty in producing a compact design made them unsuitable to be used as an optical source. Also,since the lasing medium was gas or a chemical substance, the efficiency of the medium to produce a constant output power signal degrades over time.The invention of the Solid state lasers, which are compact lasers,the design of the optical source became more simpler. While the solid state lasers produce a high powered output signal, they need to be pumped by another semiconductor laser and can provide kilowatts of output power and hence are very useful to establish deep space optical links with link distances up to 40,000kms. Though the power consumed is relatively less than the gas lasers, they still required large Amps of current to be turned on. The next category of lasers that were successfully experimented with and have been used to establish multiple crosslinks

are the Semiconductor Lasers. Driven by a current source, they are the most compact

of all the lasers used as an optical source. Several categories of semiconductor laser

diodes exist such as the Vertical Surface Cavity Emitting Laser, Quantum Cascade

Laser, Distributed Feedback lasers and Fabry Perot Lasers. All these lasers use a

semiconductor medium as the lasing medium but the process of lasing differs from

one laser to another. For a detailed discussion lasers the reader is referred to [1, 8, 9].

From the previous discussion, it can be seen that the large satellite have a number of

options when it comes to making a choice for the optical source. The same doesn't

apply to the case of the CubeSat as the options are limited only to the different types of

semiconductor laser diodes. The following sections describe the requirements to be met

by the optical source and the modulation schemes that can be used.

2.1.1 Choice of Laser Diode

A laser diode is chosen depending on the required output power and wavelength.

The average output power is dependent the distance at which the inter satellite

links needs to be established and the available drive current. For CubeSats, drive

currents values of >10mA and less than 1A for the payloads are available. Such small

currents are sufficient to drive the laser to produce optical output powers in the range

of 10mW-25mW. Since both CO_2 and solid state lasers cannot be used due to their

volume, weight and power constraints [10], the only choice of diodes that can meet

payload requirements of the Cubesats are the semiconductor laser diodes such as

Distributed Feedback laser diode (DFB), Vertical Surface Cavity Emitting Laser diodes

(VSCEL) and QCL Some of the common laser diodes and their operating wavelength

are tabulated in table 2-1.

Table 2-1. Laser diode wavelengths[1],[2]

Type of Laser Diode	Wavelength(um)
Diode Pumped Nd:YAG(YAG)	0.503-1.064
Indium Gallium Arsenide Phosphide (InGaAsP)	1.3-1.5
Aluminium Gallium Arsenide (AlGaAs)	0.8
VSCEL	0.75-1.050

2.1.2 Operation

The chosen laser diode is turned on by the bias current. In order to obtain a modulated output; the modulating current is superimposed on the bias current. The output of the laser diode is then passed through a collimator which produces a beam of the desired quality. The design of the laser diode transmitter package must meet the specified volume and weight constraints of the payload.

2.1.3 Optical Requirements

Beam Quality: The parameter of major interest from the point of view of the optical design is the beam quality which specifies how tightly or how divergent is the beam of the laser diode transmitter package. A good optical link design ensures that the beam divergence is as minimum as possible. This parameter is determined by both the laser source and collimation optics.

Minimizing Wavefront Error: The inherent astigmatism of the laser diode has to be corrected by dedicated means like cylindrical lenses to achieve the specified demanding figure of Wavefront Error (WFE) [3],[1]. Higher order deviation from the laser diode wavefront from the ideal plane wave cannot be compensated. A good correction of aberrations for the collimator itself is required to cope with the specification.

Link Establishment: For a transceiver system, the stability of the beam direction is related to the requirement on co-alignment between the transmitter and received beam in the optical terminal. The alignment cannot be made during communication and hence has to be made before the communication starts. The optical devices that are the part of the system have to maintain a stable alignment of the optical signal for a typical communication period say for 24hrs.

2.1.4 Optical Design

Collimator specifications: The optical design consists of determining the specifications of the collimator which include the focal length and numerical aperture based on the beam diameter and the e2 divergence angle. An example of a collimator

assembly is shown in figure 3. The optical design of the collimator is very demanding due to the combination on various requirements such as chromatic aberrations, optical field and wavefront error. For the example collimator assembly shown in figure 2-1, the first six lenses are used for obtaining the desired beam width and have to be manufactured with thickness +/-0.05mm. Tolerance values for air gaps +/-1um. The collimator lenses should be fully achromatized for the wavelength specified [3].
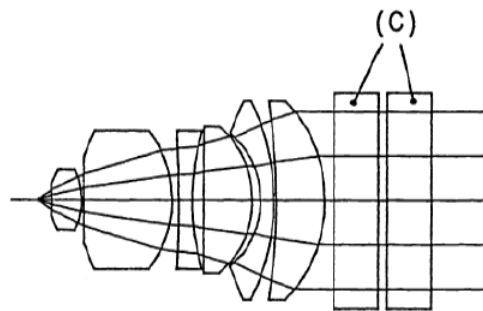
Figure 2-1. Collimator design

Compensation of aberrations: Aberrations which are produced due to the deviation of the laser source from the principle axis of the collimator have to be compensated by providing for the lateral displacement of the lenses.

Efficiency of the laser diode: If the efficiency of the laser diode drops, the drive current has to be increased, thereby causing an increase in the dissipated heat and the temperature gradient in the heat sink of the laser diode. The change in the temperature gradient causes a lateral displacement of the laser diode beam waist and the displacement has to be compensated by the terminal pointing assembly at the same maintaining the beam quality.

Astigmatism: Laser diode astigmatism has to be corrected by placing a pair of cylindrical plano convex lenses in front or behind the collimator. The lenses have to

be rotated to compensate the amount of astigmatism present. In figure 4, the lenses marked as 'c' are used for correcting the astigmatism.

2.1.5 Electrical and Mechanical Requirements

Rise Time: The rise time of the pulse is determined from the data rate to be achieved. For a data rate of 120Mbps, using QPM, a pulse width of 4ns with rise times of of 1ns have been achieved.

Frequency Response: The frequency response of a transmitter is a function of the drive current speed and the impedance matching between the laser driver output and the Laser Diode Transmitter Package (LDTP) input. The laser driver output and the LDTP input has to be properly matched as the resistance at laser diode input is smaller than the output of the laser driver. If they are not properly matched, reflections of the driver signal can occur. Also, the inherent inductance of the laser diode package has to be minimized

Operating temperature: The operating temperature of a laser diode can vary anywhere from 20 degree Celsius-100degree Celsius. The temperature at which the laser meets the power budget requirements must be chosen and maintained.

Mechanical Design

The Mechanical design has to take into consideration the following important aspects:

- Accommodation of the collimator and the cylindrical lenses for correcting astigmatism.

- Small lens diameters resulting in small dimensions of the housing.

- Positioning of the laser diode relative to the collimating optics.

The material for the lens should be chosen so as to have a high coefficient of thermal expansion. Each optical component has to have its own mount as they have to be individually centered. A laser diode support is used for mounting the laser diode relative to the collimating optics.

Electrical Design

The electrical design has to take into consideration the following important aspects:

Protection against negative current: In order to provide protection against negative current a monitor photo diode (MPD) has to be included in the laser diode package. A Schottky diode needs to be connected in parallel to the laser diode to protect it from negative current surge and a thermistor has to be positioned near the laser diode baseplate in order to measure the temperature of the laser diode with a high accuracy.

Impedance Matching: As high speed modulation is required, the two lines for modulation current and for monitor diode current have been matched to the required impedance. The drive line should have the same impedance as the resistance of the laser diode, which is around 2 Ohm. Since this very low value cannot be realized and a compromise of 10 Ohm has been chosen. The laser driver, which is matched to the 10 Ohm line, has to absorb the reflections induced by the laser diode [3], [1]. The monitor current line has standard 50 Ohm impedance. The above mentioned impedances can change depending on the resistance offered by the different types of diodes. The parameters of a Laser Diode Transmitter Package originally designed for large satellites that meet the volume, weight and power constraint for the small satellites is outlined in the table 2-2.

2.1.6   Modulation Schemes

The communication processing electronics determine the type of modulation that has to be applied to the laser. Conversely, it controls the modulator which in turn modulates the laser based on the input from the electronics. Data rates achieved with an ISL in geostationary orbit with a separation of 40,000 kilometers are about 360-500Mbits/sec. The common and simplest modulation techniques are On and Off keying (OOK), Q-ary PPM (Quaternary Pulse Position modulation) and Frequency Shift Keying (FSK).

Table 2-2. Laser diode parameter summary [3]

Parameter	Range
Clear Aperture	9mm
Wavelength	0.8um-1.064um
Transmittance	95.00%
Stability of beam direction	5urad
Wavefront Curvature Radius	250m
Wavefront Error	1/20 waves
Spectrum Width under modulation	4nm
Polarization Purity	1/100
Average Output Optical Power	30mW-400mW
Peak Optical power(DC=25%)	Depends on the diode specs
Rise Time in Pulsed Operation	For 120Mbps,pulse width is 4ns and
Depends on data rate	rise time is 1ns.
Operational Temperature Range	20-30 degrees
Dimensions	53x50x57mm
Weight	180g

2.1.6.1   On and Off Keying

Amplitude Shift keying is a form of modulation that represents digital data as variations in the amplitude of a carrier wave. The amplitude of an analog carrier signal varies in accordance with the bit stream, keeping frequency and phase constant. On and Off Keying (OOK) can be considered to be a special case of ASK where in the binary bit '1' is represented by the presence of a carrier and binary '0' is represented by the absence of a carrier signal. A variant of On and Off keying is the Non-Return to Zero scheme wherin, binary 'O' is represented by a low power signal rather than the absence of the signal. **Advantages**: The circuitry for OOK is relatively very simple and inexpensive. **Disadvantages**: It is very sensitive to atmospheric noise, distortions and propagation conditions. For Laser diodes, binary 1 is represented by a short pulse of light for a specific duration and binary 0 is represented by absence of light for a specific duration. An example of OOK is shown in figure 2-2.

2.1.6.2   Pulse position modulation

Pulse-position modulation (PPM) is a form of signal modulation in which M message bits are encoded by transmitting a single pulse in one of the 2M possible time-shifts.
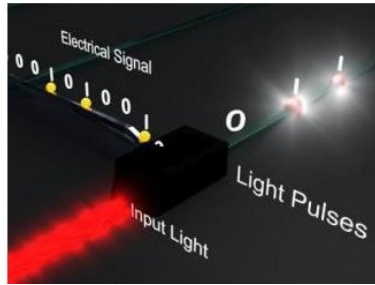
Figure 2-2. OOK modulation

This is repeated every T seconds, such that the transmitted bit rate is M/T bits per second.

Operation: It is often implemented differentially as differential pulse-position modulation, where by each pulse position is encoded relative to the previous , such that the receiver must only measure the difference in the arrival time of successive pulses. It is possible to limit the propagation of errors to adjacent symbols, so that an error in measuring the differential delay of one pulse will affect only two symbols, instead of affecting all successive measurements.

Advantages: One of the principal advantages of PPM is that it is an M-ary modulation technique that can be implemented non-coherently, such that the receiver does not need to use a phase locked loop (PLL) to track the phase of the carrier. This makes it a suitable candidate for optical communications systems, where coherent phase modulation and detection are difficult and extremely expensive.

Disadvantages: A key difficulty of implementing this technique is that the receiver must be properly synchronized to align the local clock with the beginning of each symbol. Aside from the issues regarding receiver synchronization, the key disadvantage of PPM is that it is inherently sensitive to multi path interference that arises in channels with frequency-selective fading, whereby the receiver's signal contains one or more echoes of each transmitted pulse. Since the information is encoded in the time of arrival (either differentially, or relative to a common clock, the presence of one or more echoes

can make it extremely difficult, if not impossible, to accurately determine the correct pulse position corresponding to the transmitted pulse.

2.1.6.3 Frequency Shift Keying

Frequency-shift keying (FSK) is a modulation scheme in which digital information is transmitted through discrete frequency changes of a carrier wave. The simplest FSK is binary FSK (BFSK). BFSK uses two discrete frequencies to transmit binary (0s and 1s) information. With this scheme, the "1" is called the mark frequency and the "0" is called the space frequency. In Optical communications, a variation of FSK known as M-FSK is used where in 2 or more frequencies are used to binary data.

Disadvantage: The laser diode needs to be tunable to a wide range of frequencies for FSK to be used and this would cause the laser diode to deviate from its central wavelength over time.

To summarize, on off keying and Non Return to Zero can be implemented with simple circuitry when compared with PPM and FSK with penalty of smaller data rate when compared to FSK and PPM.Also PPM and FSK require stringent clock synchronization techniques since coherent demodulation and not direct detection is the primary method to demodulate the received signal. Hence the candidate modulation scheme is ON OFF keying or NRZ.

2.2 Optical Detector

The optical detector is the receiving element that converts the optical signal into an electronic signal. The electronic signal is further sent to the demodulating electronics that retrieve the original transmitted signal. The four important optical detectors are the PIN diode, APD, CCD and CMOS detectors. The detectors are characterized two main parameters namely quantum efficiency and responsivity at a specific wavelength. Quantum efficiency of a detector is the ability to generate electrons for every incoming photon and responsivity is amount of electric current generated per watt of incident optical power. Detectors operate in a reverse biased mode and hence have high

operating voltages in the range of 15-30V. While the PIN diodes have a responsivity in the range of 0.5-0.7A/W and low operating voltages and are used for short link distances the APDs have a responsivity in the range 0f 20-80A/W and higher operating voltages and are used for long link distances. As with pin photo diodes, silicon APDs can be used in the wavelength range of 300 nm to approximately 1050 nm. For 800 nm to 1700 nm, InGaAs diodes are available. Charge coupled devices (CCDs) and CMOS focal plane arrays could be considered as receive elements, too. Both are available in one-dimensional and two-dimensional configurations with up to a few thousand pixels in one dimension. The major drawback of this technology is the limited pixel readout frequency of some 10MHz. Assuming a line sensor with 100 pixels and a pixel clock frequency of 10 MHz, a maximum data rate of 100 kbit/s and an angular resolution on the order of 1/100 of the field-of-view could be achieved. Another disadvantage is the large amount of readout electronics required (with its extra power consumption) [11].

Using optical preamplification can improve the performance of receivers. When direct detection without preamplification is used, the only sources of noise are background noise,detector dark noise and electronic amplifier noise [12]. The electronic amplifier noise is negligible when compared with the other two noises. With optical preamplification, several noise sources such as Signal Shot noise,Amplified Stimulated Emission, Spontaneous Beat Noise etc are prevalent. Optical preamplifiers if required are available as fibre amplifiers or as semiconductor optical amplifiers. Use of these amplifiers again adds to the weight and power consumption of the system and hence should be incorporated into the design only when absolutely necessary.

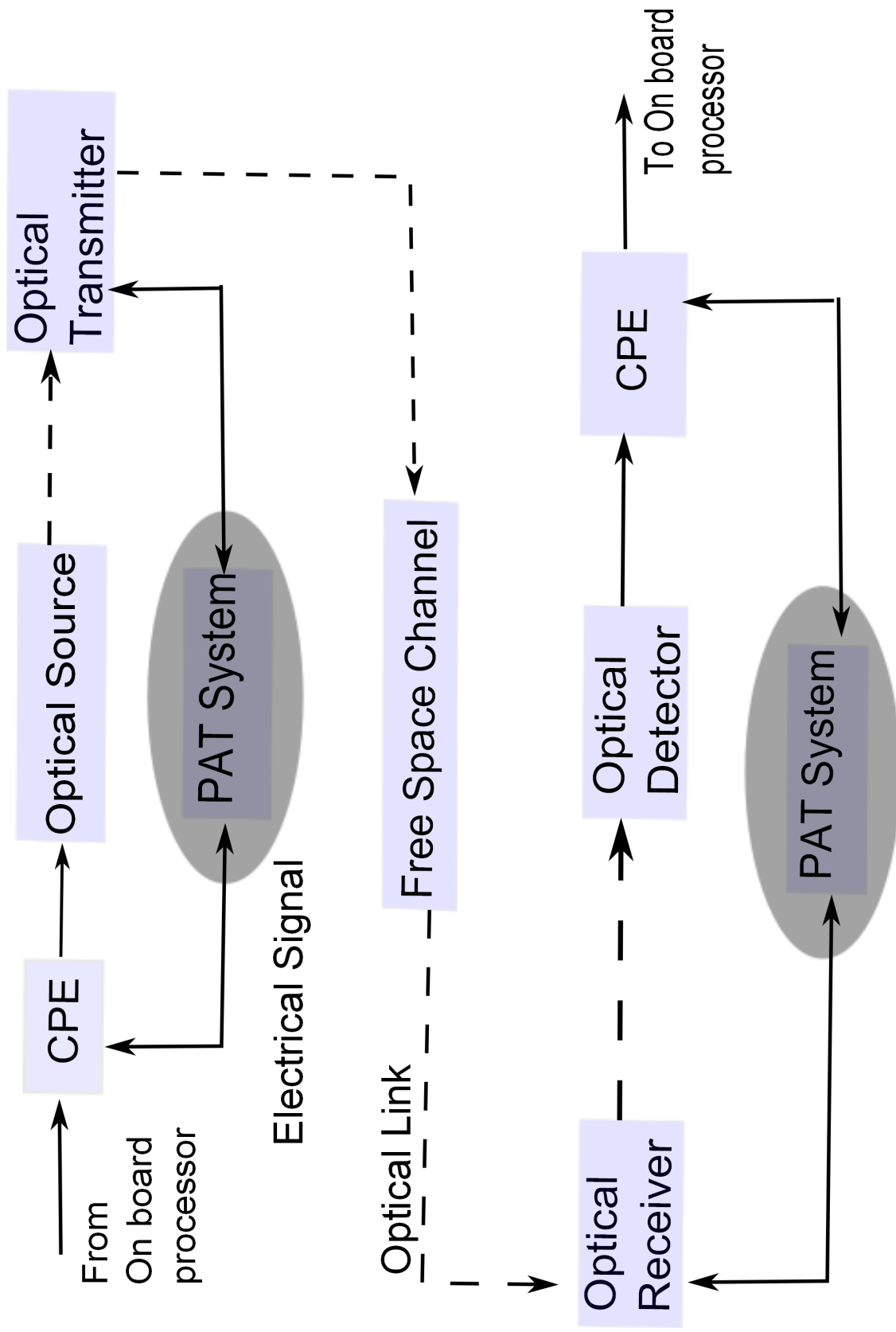To provide background suppression and channel selection (the latter in WDMA systems only), an optical bandpass filter has to be used at the receiver input. In general, wide field-of-view, narrow bandwidth, and low insertion loss are contrary requirements and a compromise will have to be found among them. Thin film interference filters are available with bandwidths down to 1 nm, their transmission varies from 60% for

Table 2-3. Operating wavelengths of optical detectors

Material	Wavelength(nm)
Silicon	190-1100
Germanium	400-1700
Indium gallium Arsenide	800-2600
Lead II sulphide	<1000-3500

the narrow types to around 90% for filters with several 10 nm bandwidth. The center wavelength of a dielectric Fabry-Perot filter shifts with angle of incidence by some 1 to 2 nm/, thus limiting the passband for wide-field-of-view applications. Due to their minimal angular dependence and low transmission loss, absorption filters based on GaAs are an attractive alternative to interference filters. Table 2-3 gives the operating wavelengths of some of the detectors.

Figure 2-3. ISL block diagram

Optical Transmitter

Optical Source

PAT System

CPE

From On board processor

Electrical Signal

Free Space Channel

Optical Link

To On board processor

CPE

Optical Detector

PAT System

Optical Receiver

CPE- Communications Processing Electronics   PAT:Pointing, Accquisition & Tracking

CHAPTER 3
POINTING, TRACKING AND ACCQUISITION ASSEMBLY(PAT)

The Pointing, Acquisition and Tracking subsystem consists in acquiring and tracking the counter terminal incoming laser beam as well as in pointing the transmitter terminals outgoing beam with an accuracy which enables data transmission between two satellites. The operations that are needed to be carried out by the subsystem consist of [13],[14],[15] :

- Acquisition phase which has to compensate for the initial beam pointing error due to spatial acquisition errors, mainly ephemeris error and spacecraft location prediction errors.

- Tracking phase wherein once the beam is acquired, it has to track out local angular disturbances transmitted from the host platform and the dynamic elements of the payload with submicroradian accuracy.

- Pointing phase wherein the terminal's optical head is pointed towards the opposite satellite after compensation for relative platform motions and finite transit time of light.

For large satellites, due to the less stringent space and power constraints, each of the three tasks are performed by separate systems. Acquisition is performed by the acquisition system,the tracking phase carried out the coarse pointing system and the pointing phase carried out by the fine pointing system. Each system in turn its controlled by a different electronic system such as the Acquisition Processing Electronics, Coarse Pointing Electronics and the Fine Pointing Electronics. For detailed discussion on these systems, the reader is referred to [3, 13, 16–20]. These large systems are very necessary to establish long distance and deep space optical links and hence cannot be done away with for large satellites. Since we are aware of the constraints of the CubeSat, we can work with the assumption that a single system would suffice to satisfy the PAT needs of the CubeSat.

In order to carry out the PAT tasks for the CubeSat, the PAT system should be able to orient the optical element directing the optical signal along its x and y axis. There are two possible devices to carry out this task.

- An electro mechanical device that can provide torque to the gimbaled optical device.

- A MEMS mirror that can be used to direct the optical signal in the required direction.

While the MEMS mirrors can be subject to radiation wear and tear, the more robust option is to go for the electromechanical device which is the subject of further discussion.

3.1   Pointing, Acquisition and Tracking Strategies

3.1.1   Acquisition Strategy

To establish a link to start communication between two satellites S1 and S2, the satellite S1 must send out a beacon signal. The divergence of the beacon signal is limited to say 700urad. The cone of uncertainty could be limited to 8000urad. The satellite S2 scans the cone of uncertainty till its terminal is illuminated by the laser beam. Once illuminated, it must detect the direction of the incoming light, correcting its Line of Sight, start tracking and emits its communication beam towards the transmitting satellite. Once the satellite S1 receives the communication beam from S2, it stops sending its beacon, starts tracking and corrects its line of sight and sends its communication beam [9],[13]. The two satellites are now in mutual closed loop tracking.

3.1.2   Tracking and Pointing Strategy

The extremely high pointing accuracy of 1 microrad is met by using the incoming light from the counter terminal as a reference to the pointing actuators. The two terminals are thus in a co-operative closed tracking loop during communication. The tracking angle corresponds to where the tracked terminal was when the light was emitted whereas the ideal pointing direction corresponds to where the pointed terminal will be when the light arrives, i.e. the pointing angle must be offset with respect to the
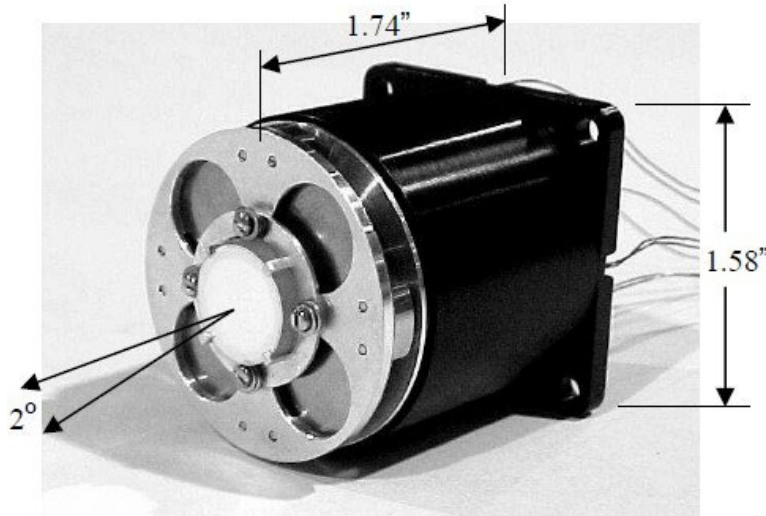
Figure 3-1. PAT assembly

tracking reference with the so called point ahead angle (due to relative transverse satellite velocity and the finite velocity of light) [14].

The PAT assembly is shown in figure 3-1 provides deflection of the incoming and out coming laser beams around two orthogonal axes and thus performs the following operations:

- In the scanning mode, it sweeps the beacon over a wide angular range.

- In the acquisition mode it provides a fast deviation angle over a wide range to re center the incoming beam on the tracking sensor as sensed by the acquisition sensor.

- In the tracking mode it controls of the angular position of the incoming beam as sensed by the tracking sensor with high bandwidth and accuracy.

The design specifications of the PAT assembly detailed as follows:

Positional Accuracy: The distance between the satellites may be several thousands of kilometres. To establish a link between two satellites that is in order to point the laser beam onto the mirror of the other satellite, requires a positional accuracy of 1urad. The device should also be able to move the mirror by +/- 2 degrees to provide coarse pointing around the neighbouring satellite .

Bandwidth: The device must have sufficient bandwidth to reject satellite vibrations and disturbances. For small signal disturbances on the order of 0.01 degrees, this bandwidth should be about 200 Hz. Larger disturbances of about 1 degree need to be rejected below 1 Hz [15] .

Actuating the mirror: Two types of devices are usually considered for actuation of the beam-steering mirror: voicecoils and piezoelectric actuators. The former offers a potentially large stroke for little power input, but is somewhat limited in bandwidth due to its low force output and consequently low stiffness. Piezoelectric actuators by contrast offer high bandwidth and stiffness, but provide very small position output even at relatively high voltages. The ideal device should combine the benefits of both technologies. While performing all the above described functions the power consumption of the device should be very low [13],[15]

3.2   PAT Algorithm

An example acquisition algorithm is shown in figure 3-2, where the transmitter beam is widened such that it illuminates the receiver from any position within the area of uncertainty . At the beginning of the acquisition process, the receive antenna points at the center of the area of uncertainty Then it starts the spatial search by sequentially scanning the uncertainty area along a spiral track. When the transmitter is found, the receiver switches into tracking mode, where a spatial tracking loop is closed by evaluating the signal from a position sensitive detector and using this information to control the alignment of the optical antenna. The transmitter beam divergence is not reduced during this tracking mode [14],

3.3   Electro Mechanical Design Choice

A design example of a PAT system that meets the 3U CubeSat specifications is briefly summarized in [15] . It is essentially a configuration of four identical electromagnetic circuits, positioned at 90 degrees from each other around the circumference of a circle as shown in figures 3-3 and 3-4. Four small permanent magnets are mounted to a
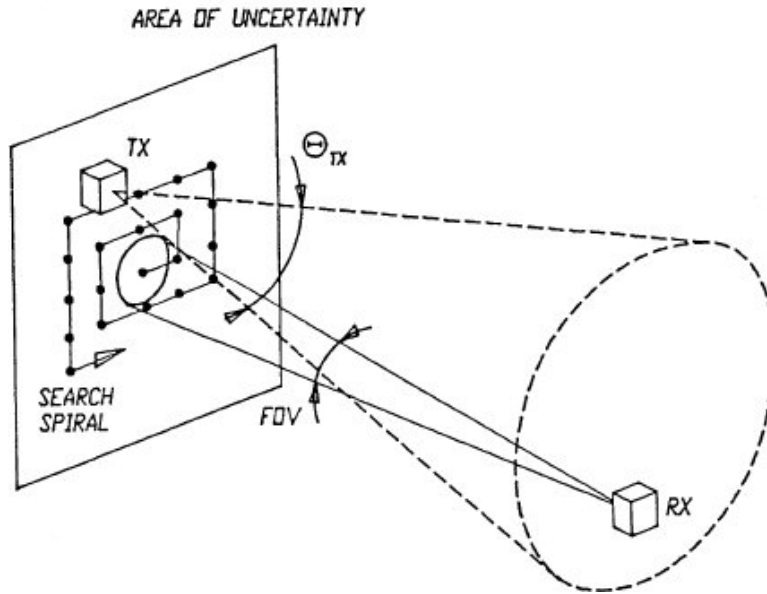
Figure 3-2. PAT algorithm

moving mirror platform, while four corresponding coils and coil cores reside within

a fixed housing. Consequently, most of the components are stationary. Each circuit

magnetically pulls on the mirror platform. However, by increasing positive current in one

coil a magnetic field is generated which opposes that of the permanent magnet directly

in front of it. Simultaneously increasing negative current in the coil 180 degrees away

adds to the magnetic field in that circuit. In this way, a differential force is produced

which tilts the mirror platform about its center. Similar operation of the other two

coils produces motion along the orthogonal axis, so that the mirror can be positioned

anywhere within an optical cone. The platform is mounted on a flexible BeCu diaphragm

that provides a linear restoring torque in any direction against which the electromagnetic

torque can react, yielding positional control. Also, by varying the total current in all

four coils simultaneously, the platform can be positioned linearly along its center line,

providing an additional degree of freedom if desired. The parameters of the described

PAT system are tabulated in table 3-1

Table 3-1. PAT parameters

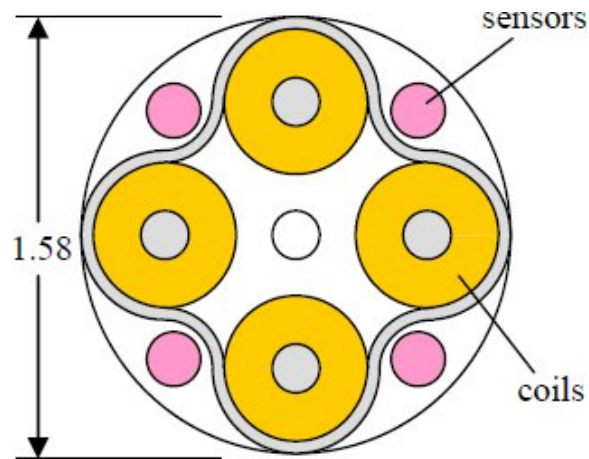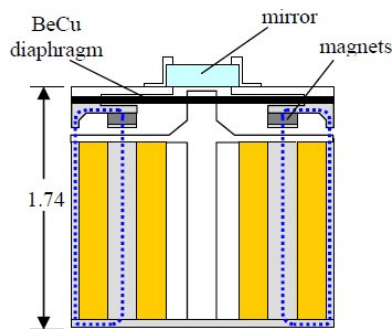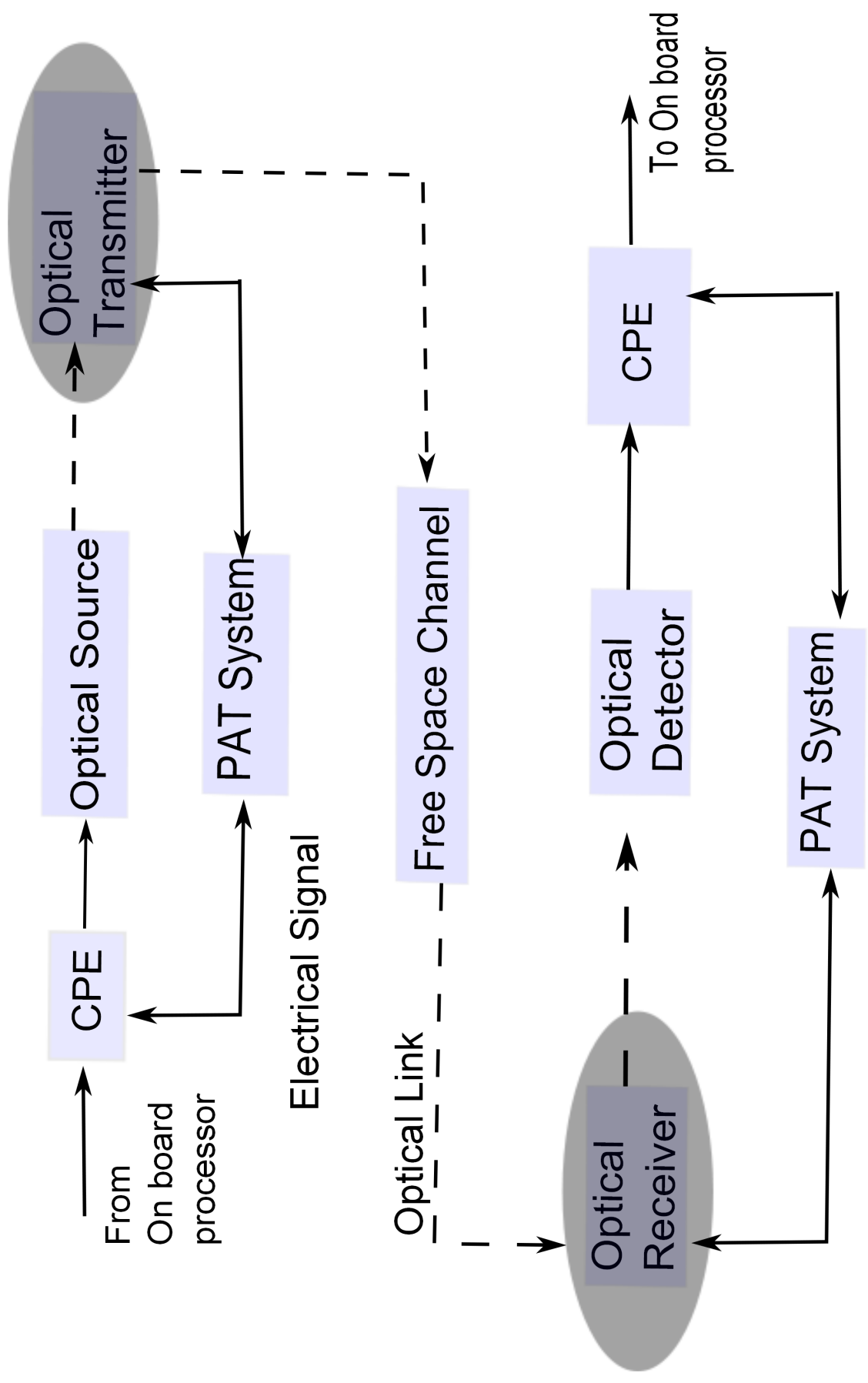| Parameter	Range
Maximum Deflection range	+/- 35000microradians
Bandwidth	200Hz for disturbances of 0.01 degrees 1Hz for disturbances of 1 degree
Dimension	Less than 3 inches in length, breadth, height and diameter.
Weight	400gms-250gms
Power	1.5 watts in tracking mode 5-16 watts in acquisition mode

Figure 3-3. Top view cross section of PAT system.

Figure 3-4. Side view of cross section of PAT system

Optical Transmitter

Optical Source

PAT System

CPE

From On board processor

Electrical Signal

Free Space Channel

Optical Link

Optical Receiver

Optical Detector

PAT System

CPE

To On board processor

CPE- Communications Processing Electronics   PAT:Pointing, Accquisition & Tracking

Figure 3-5. ISL block diagram

CHAPTER 4
TRANSMITTER AND RECEIVER

The optical transmitter is the most important component of the laser communication system as it performs the following two major functions. First, it is used as a launchpad for the optical signal and in doing so must preserve the optical quality of the signal Second, it acts as a means to focus the incoming signal onto the imaging optics which in turn relay the signal to the optical detector. Larger systems use a single instrument to transmit as well as receive the signal, while smaller systems make use of different instruments for transmission and reception of the signal. The telescopes used in the large satellites can be used to construct the transmitter and receiver for the small satellites too. However, the specifications have to be tailored to meet the design constraints of the small satellites. In this chapter, we explore the various configurations of telescopes along with their merits and demerits. The candidate telescope is selected and the specifications are outlined for the small satellite. The telescopes for the laser communication system (LCS) system are derived from the various common astronomical telescopes and their characteristics are summarized as follows [21].

4.1   Common Astronomical Telescopes

4.1.1   Off-Axis Newtonian

The off axis newtonian telescope consists of a off-axis paraboloidal mirror cut out of a larger paraboloidal parent mirror as shown in figure. The off-axis characteristic produces a telescope that is unobstructed as neither the transmitting or receiving signal is blocked and hence the instrument doesn't play a role in degrading the quality of the signal. A deflecting mirror is employed to direct the signal towards the telescopes for transmission or away from the telescopes where it can be conveniently handled by the imaging optics. Since the off axis mirror is in fact a part of the larger paraboloid,
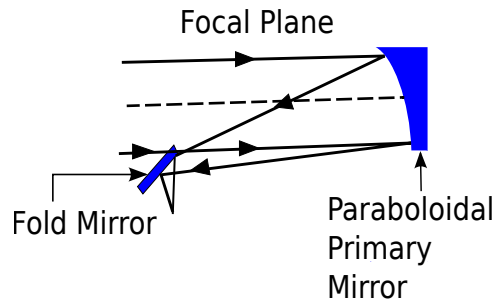
Figure 4-1. Off-Axis Newtonian

reducing the focal length of the mirror cannot be carried out without degrading overall optical image quality as very short focal mirrors are very difficult to manufacture.

4.1.2 Cassegrain

The cassegrain configuration consists of a paraboloidal primary mirror and a hyperboloidal secondary mirror. The configuration is very compact due to the folding employed and the length of the telescope can be as much as one-third the focal length of the telescope. Since the configuration consists of two mirrors, the placement of the secondary with respect to the primary is very critical and tolerances of the order of fractions of a thousandths of an inch are common. The fact that the design consists of two mirrors produces a field of view of half a degree and wavefront qualities of lambda/16 rms have been produced in the past. The secondary diameter is 0.2 to 0.25 of the primary diameter.

4.1.3 Off-Axis Gregorian

The off-axis Gregorian telescope is as shown in figure 4-3. As can be seen, the optical signal is focused before being incident on the secondary mirror. The point of focus can be used to insert a field stop which determines the field of view (FOV) of the telescope. Also a Lyot stop can be inserted at the point as shown to reject stray light reflected from tubes, baffles or edges of the primary mirror. The off-axis Gregorian telescope thus combines the unobscured characteristic of the cassengrain telescope
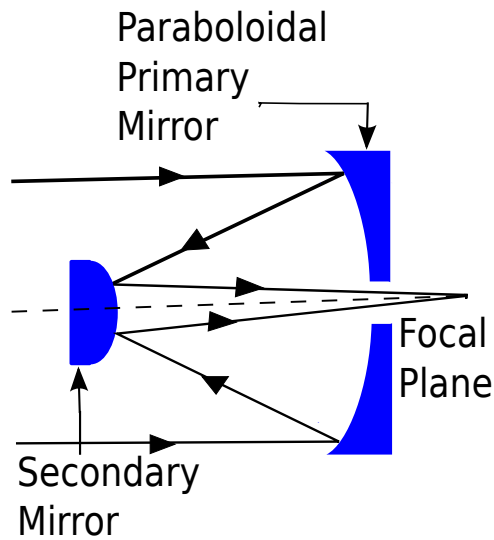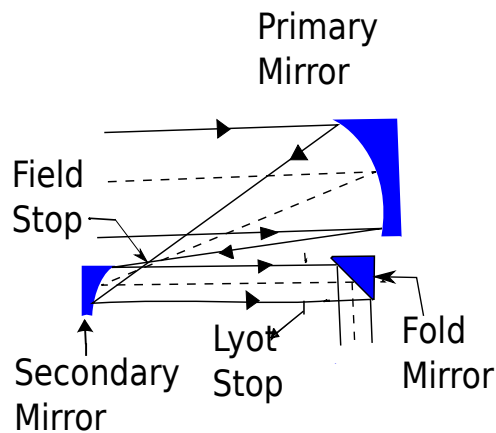
43

Figure 4-2. Cassegrain

Figure 4-3. Off-Axis Gregorian

and the Gregorian stray light rejection capability thus making it a good candidate for a crosslink telescope.

4.1.4 Cassegrain with Refractive Elements

In order to increase the FOV of astronomical telescopes, refractive elements are added to the Cassegrain telescope as shown in the figure. Telescopes with refractive elements are called catadioptric, i.e they combine reflective(catoptric) elements with refractive (dioptric) elements. Currently, telescopes make use of doublet and triplet lenses to increase the FOV.
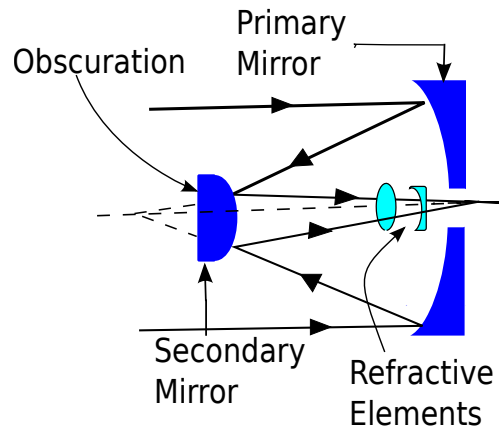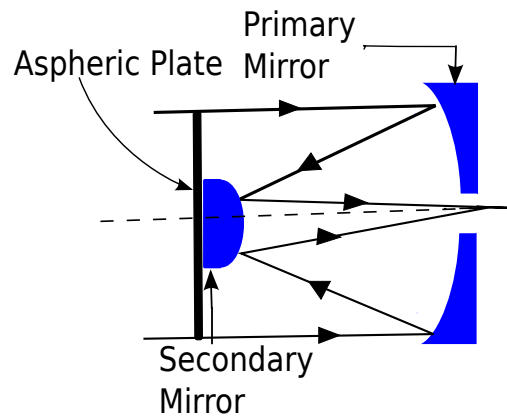
Figure 4-4. Cassegrain with refractive elements

Figure 4-5. Schmidt-Cassegrain

4.1.5   Schmidt-Cassegrain

This telescopes is a combination of a Schmidt and Cassegrain design. The schmidt design makes use of an aspheric plate to correct spherical abberations and when combined with a Cassegrain a large flat field telescope. A field of greater than 1 degree is available with diffraction limited performance.

4.1.6   Maksutov-Cassegrain

The Maksutov-Cassegrain is a wide field of view catadioptric telescope.It produces FOV of 10's of degrees but with a disadvantage of a spherical focal plane. A flat-field telescope with a less ambitious FOV can be produced with a Cassegrain two mirror configuration, a field similar to the Schmidt-Cassegrain. For larger apertures, the
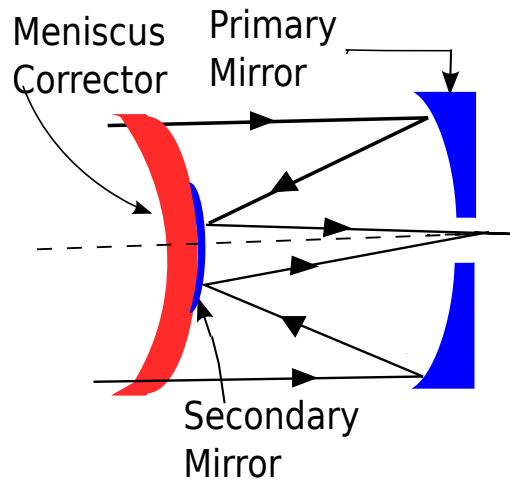
Figure 4-6. Maksutov-Cassegrain

meniscus corrector is heavier for the same size telescope than a corresponding

Schmidt plate. With proper design parameters assigned during the design process,

the secondary can be placed on the spherical corrector plate by the simple expedient of

reflectivity coating the center of the plate as illustrated. The radius of the secondary is

the same as the back side of the meniscus corrector. These telescopes are of extremely

high quality of about (λ/40) rms.

4.2   Telescope Characteristics

The following section describes some of the important telescope characteristics and

their influence on the construction of the telescope for a LCS terminal. A summary of the

characteristics of the telescopes described is tabulated in 4-1.

4.2.1   Variation of f/#

The position of the image formation plays an important role in deciding on the type

of telescope that is to be used in a LCS terminal. The Cassegrain telescope and its

variants produce images that are behind the primary and hence makes it convenient

to handle the incoming signal. The Cassegrain f/# or f number is the the ratio of the

focal length to the aperture of the telescope and typical numbers for the Cassegrain

telescope range from f/8 to f/15 and the primary f/# may range from f/8 to f/1.5. The

shorter primaries are faster and more difficult to manufacture while a t the same time

resulting in a shorter telescope and the longer primaries are slower resulting in a longer telescope.

Table 4-1. Telescope parameter summary [1]

Figure Number	Central Obscuration	FOV	Relative length	Internal Field Stop	Relative Weight	Tube
4-1	No	Upto $1/4^o$	Long	No	Light	Open
4-2	Yes	About 12°	Short	No	Medium	Open
4-3	No	About $1/2^o$	Long	Yes	Medium	Open
4-4	Yes	$> 1^o$	Short	No	Light Medium	Open
4-5	Yes	$> 1^o$	Short to Medium	No	Medium to Heavy	Closed
4-6	Yes	$> 1^o$	Medium	No	Heavy	Closed

4.2.2 Resistance to Jamming

Crosslinks employed in military operations must be jam resistant.Jamming is the process of interfering with a signal by transmitting another signal with similar properties such as modulation, right wavelength and power. The jamming can take place by interfering with the acquisition, tracking or communication processes. The ability of the crosslink system to resist jamming is called off-axis rejection and the most useful value to quantify this property is called point source rejection or PSR. PSR is the ratio of the energy incident on the receiver to the energy entering the telescope at the angle of interest. There are several techniques available to increase the PSR. Some of them summarized below:

- To shield the primary at larger off-axis angles.

- Use of internal baffle surfaces of very low reflectance on the order of a few percent.

- The primary mirror has to be smoothly polished.

- A reimaging group of lenses is used following the telescope which permits the incorporation of a field stop or lyot stop.

- The design of the telescope is very important. Some telescopes are designed for off-axis rejection. Such an example is the off-axis Gregorian since there is no secondary or no spider, and the presence of a field stop has the effect of eliminating extraneous off-axis light.

- The small FOV, the better the rejection of stray light. For example, a system with a 100urad FOV has 100 times better stray light rejection than a system 100mrad FOV.

4.2.3 Diffraction Limited Telescopes

The term diffraction limited is generally associated with the Rayleigh quarter wave criterion, which means that any telescope or any optical element also that exhibits a wavefront error equal to or less than 00.075(lambda/13.3) wavers RMS can be considered to be diffraction limited. It is referenced to the wavelength of interest.

To achieve diffraction limited performance in a telescope after it has been installed in satellite, launched and on-orbit for years while under the influence of temperature swings, thermal gradients, material instabilities is no easy task. The design must be exact, the materials chosen must be suitable for the task, the manufacture and alignment must be perfect and finally the environment in which the telescopes must operate need to be well understood and controlled to appropriate limits. The telescopes forms the transmit beam and any errs in the figure will degrade the beam quality,thus weakening the received signal a the companion terminal. For some telescopes, a window across the aperture may be desirable for rejection of sunlight by use of an appropriate solar rejection coating. The direct impingement of the sun on the primary can cause severe distortion with resulting transmit signal loss. Resistance to a laser weapon threat may also be increased.

4.2.4 Telescope Materials

Telescope lenses once constructed are housed in a cylindrical tube made from one the materials listed in table 4-2. The other important properties of materials such as

Table 4-2. Telescope material densities [4]

Material	Density gm/cm^2
Beryllium	1.85
Aluminum	2.70
ULE	2.20
Glass	2.53
Fused Silica 2.02	
Zerodur	2.53
Invar 36	8.03
Titanium	4.43
SXA(Al)	2.91
Graphite Epoxy	1.78

Table 4-3. Telescope parameters

Parameter	Value
Aperture	10cm
Weight 1.85gm/cm^2	1kg-2.4kg approx
Primary mirror focal length(f/4)	40cm
Primary mirror focal length(f/1.5)	15cm
Secondary mirror diameter	2.5cm
Field of view	$1/2$ degree

Expansion Coefficient, Thermal Conduction, Elastic Modulus, Micro Stress Analysis, Specific Heat are not discussed as they don't contribute to the weight of the telescope and are beyond the scope of this work. Since density is the main contributor to the weight of the telescope,the material with the lightest density is considered to be used for the construction of the telescope.

On studying the astronomical telescopes with respect to their contribution to the weight of the payload, their characteristics and the materials used for construction, the Cassegrain telescope was found to provide the least weight and hence was finalized as the candidate optical transmitter. Using the specifications of the Cassegrain telescope, the optical transmitter and receiver for the small satellite would have the following specifications as listed in 4-3 based on the previous discussion.

CHAPTER 5
ANALYSIS OF THE SYSTEM DESIGN

Optical crosslinks can be established over distances as small as 10m and as large as 1000's of km. The design parameters of the subsystems were determined in order to achieve communication over long distances. Hence,for long distance crosslinks each one of the subsytem plays a vital role and cannot be removed if accurate crosslink design is a necessity.The weight, volume and EPS requirements of the proposed system are summarized in table 5-1 .In regard to the weight of system,as can be deduced from the table, the contribution to the weight of the payload from the optical source, PAT and detector is very minimal. A large part of the contribution to the weight comes from the transmitter/receiver telescopes. The transmitter and receiver telescopes are an essential device to achieve long distance crosslinks. Therefore careful consideration of the materials to manufacture telescopes should be carried out carefully.In regard to the power consumption of the system, the PAT system consumes the maximum amount of power and in the case of the detector, voltages in the range of 15-30V are hard to be generated given the very low power generation of 3W by the CubeSat. Hence though the system successfully meets the volume and weight specifications and can be compactly packed inside the CubeSat, it doesnt satisfy the power requirements. Also, it not possible to duplex link due the space constraints as a duplex link is necessary for the successful acquisition, tracking, pointing and establishment of the crosslink. It can be seen that low weight, one primary reason for which optical communications are preferred over RF for long range crosslinks is a slightly difficult parameter to achieve for the CubeSat. However, a viable alternative is to deploy the system a on 6U CubeSat as this system would not only meet the volume and weight constraints of the 6U CubeSat but also the power requirements.

However, if short range crosslinks about 1km are desired, then the subsytems such as the PAT and telescopes can be removed from the system design.It is then

Table 5-1. Optical Payload Parameters Summary

Subsystem	% Weight	Volume	EPS Requirements
Source	9	53x50x57mm	10-50mA
PAT	20	L=4.35cm H=3.95cm	1.5W-15W
Tx/Rx	50	L=15cm,H=10cm	No power consumption
Detector	Negligible	Negligible	15V-30V

assumed that the transmitter and receiver are perfectly aligned and there is no need for pointing, acquisiton and tracking of the receiver terminal for link establishment.If however, pointing, acquisition and tracking is requried, an approach in the form of a flat mirror tiltable along one or two axes in front of the terminal aperture is attractive due to the availability of lightweight electrostatically tiltable mirrors based on MEMS technology. This silicon-based technology allows to manufacture electrically driven mirrors with diameters between 300 and 2000 m with switching times as low as a few ms and angular movements between 3 and 20. (Such a system can, of course, also provide continuous pointing of narrow beams in two orthogonal directions.)The output laser power has to be sufficient to traverse the link distance without being corrupted to a undetectable level by the background noise. At receiver end, the aperture size of the photodiode which is about 5mm is sufficient to receive the transmitted signal.

CHAPTER 6
LINK BUDGET ANALYSIS

A link budget is a tool to help the communication system designer to design and analyse any communication link where the medium of transmission can be wireline or wireless and the signal for transmission of data be radio frequency or optical. This chapter describes the optical communication link design for the CubeSat using the parameters of subsytems the finalized in chapter 5 where necessary. The software used for the design and analysis of the link is the OptiSystem software.

6.1   OptiWave Software

OptiSystem is an innovative, rapidly evolving, and powerful software design tool that enables users to plan, test, and simulate almost every type of optical link in the transmission layer of a broad spectrum of optical networks from LAN, SAN, MAN to ultra-long-haul. It offers transmission layer optical communication system design and planning from component to system level, and visually presents analysis and scenarios. A simplex communication system is modelled using OptiSystem. A duplex communication system is not considered for the simulation analysis as the system design wouldn't meet the constraints of the CubeSat. The following components from the software were used to model the system are tabulated in table 6-1 .

6.2   Link budget equation

In this section we outline the link budget equations and explain each term in detail.The electrical parameter values for the RF CubeSat system and proposed Optical System are listed and the corresponding results analyzed.

$$P_r = P_t G_t L_t L_R G_r L_r \qquad\qquad (6\text{–}1)$$

where,

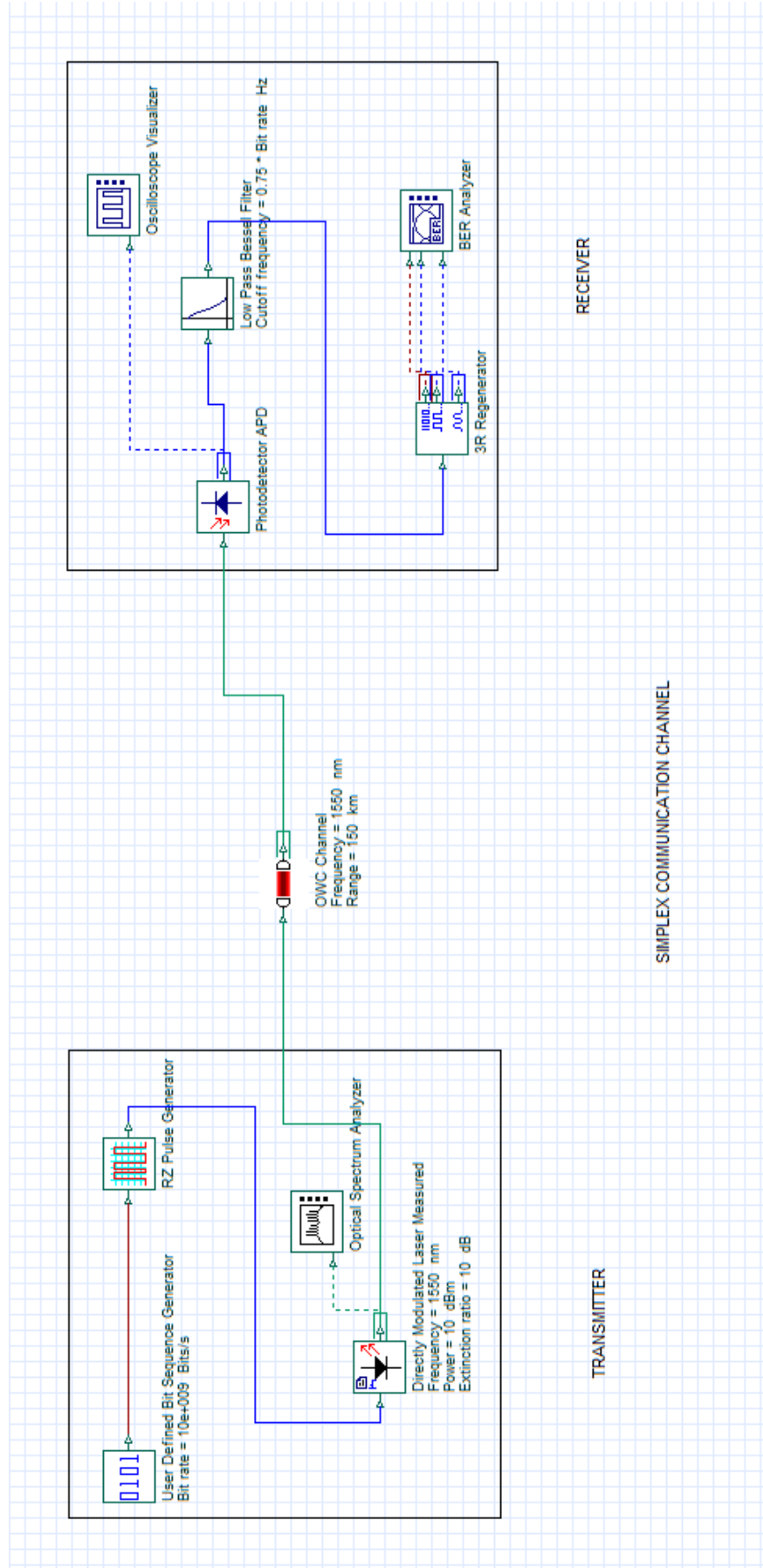P_t=Power transmitted power

G_t=Effective transmit antenna gain

Figure 6-1. Communication system

Oscilloscope Visualizer

Low Pass Bessel Filter
Cutoff frequency = 0.75 * Bit rate Hz

BER Analyzer

Photodetector APD

3R Regenerator

RECEIVER

OWC Channel
Frequency = 1550 nm
Range = 150 km

SIMPLEX COMMUNICATION CHANNEL

RZ Pulse Generator

User Defined Bit Sequence Generator
Bit rate = 10e+009 Bits/s

Optical Spectrum Analyzer

Directly Modulated Laser Measured
Frequency = 1550 nm
Power = 10 dBm
Extinction ratio = 10 dB

TRANSMITTER

Table 6-1. Components of the communication system
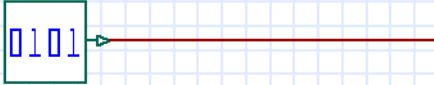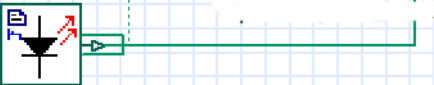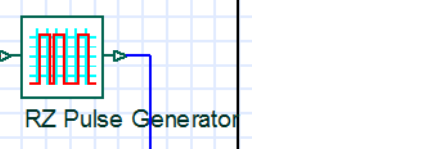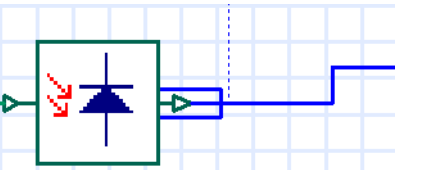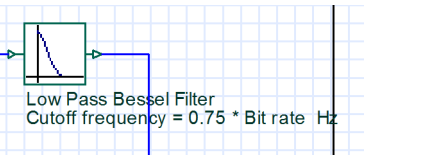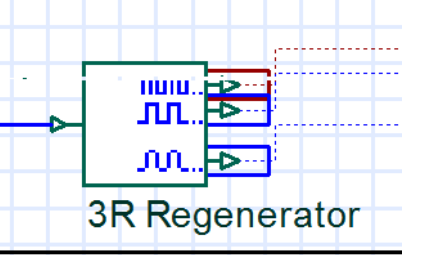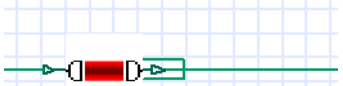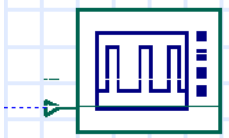
Component	Description
User Defined Bit Sequence Generator Bit rate = 10e+009 Bits/s	Generates the sequence of Bits
Directly Modulated Laser Measured Frequency = 1550 nm Power = 10 dBm Extinction ratio = 10 dB	Optical source
RZ Pulse Generator	Modulates the optical Source
Photodetector APD	Avalanche Photodetector
Low Pass Bessel Filter Cutoff frequency = 0.75 * Bit rate Hz	Filters out unwanted frequencies
3R Regenerator	Demodulates the received signal

Table 6-4. Continued

Component	Description
BER Analyzer	Analyzes the bit error rate
OWC Channel Frequency = 1550 nm Range = 10 km	Medium of Transmission of the Optical Signal
Oscilloscope Visualizer	Visualize the signal

L_t=Efficiency loss associated with the transmitter

L_R=Free space range loss

G_t=Receive antenna gain

L_r=Efficiency loss associated with the receiver

6.2.1 Transmitter Power

The transmit source power is a direct entry into the optical link equation. It is the measured signal power at the output of the laser. Usually, the transmit power is specified in watts, if the designer is consistent the average power can be used and specified in milliwatts. In case the laser is hermetically sealed, the power coming out of the hermetic

seal needs to be considered. The power at the output of the laser is given by

$$P_r(f) = H_T(f).I_d(f) \tag{6-2}$$

where H_T is the transfer function of the laser and $I_d(f)$ is the injected current in A. H_T is given by

$$H_T(f) = H_T(0).H_T^*(f) \tag{6-3}$$

Multimode Fabry Perot Laser The transfer function of a multimode fabry perot laser is expressed as [22], [23] :

$$H_T = \left(\frac{h.c}{\lambda.q}\right) . \eta_{int} . \eta_{ext} . \left[\frac{I_d - I_{th}}{I_d}\right] \tag{6-4}$$

where

$$\eta_{ext} = \frac{ln\left[\frac{1}{R_l}\right]}{\gamma.l + ln\left[\frac{1}{R_l}\right]} \tag{6-5}$$

$$\eta_{int} = \frac{\tau_{nr}}{\tau_{nr} + \tau_r} \tag{6-6}$$

$$H_T^*(f) = \frac{f_o^2}{f_o^2 - 4.\pi^2.f^2 + j\beta 2\pi f} \tag{6-7}$$

where

$$f_o^2 = \frac{(I_o - I_{th})}{\tau_{sp}\tau_{ph}I_{th}} \tag{6-8}$$

$$\beta = \frac{I_o}{\tau_{sp}I_{th}} \tag{6-9}$$

Quantum Cascade Laser The Quantum Cascade laser and Distributed Feedback Lasers are modelled using the following rate equations [22], [23]:

$$\frac{dN}{dt} = \frac{I}{q.V_{act}} - g_o(N - N_o)(1 - \varepsilon.S) - \frac{N}{\tau_n} + \frac{N_e}{\tau_n} \tag{6-10}$$

$$\frac{dS}{dt} = \gamma g_o(N - N_o)(1 - \varepsilon.S)S + \frac{\gamma\beta N}{\tau_n} - \frac{S}{\tau_p} \tag{6-11}$$

Table 6-2. Parameters of equations

Parameter	Description
I_d	Injected current
I_{th}	Threshold current
R_l	Mirror Reflectivity
γ	Loss coeficient
l	Cavity longitudinal dimension(m)
I_o	Polarization current(A)
τ_{sp}	Carrier recombination lifetime(s)
β	Dumping frequency(Hz)
f_o	Resonant frequency(Hz)

$$\frac{S}{P_f} = \frac{\gamma \tau_p \lambda_o}{V_{act} \eta h c} = \upsilon \qquad (6\text{--}12)$$

Table 6-3. Parameters of rate equations

Parameter	Description
N	Active region carrier density
q	Electron charge
V_{act}	Active region volume
g_o	Gain Coefficient
N_o	Optical transparency density
ε	Fenonmenological gain saturation term
S	Photon Density
τ_n	Carrier lifetime
N_e	Equilibrium carrier density
γ	Optical Confinement Factor
β	Spontaneous emission coupling factor
τ_p	Photon lifetime
λ_o	Lasing wavelength
η	Differential quantum efficiency per facet
h	Plank's constant
c	Velocity of Light

6.2.2 Transmitter gain

The gain of the transmitting antenna is given by

$$G_t = \frac{4\pi A}{\lambda} \qquad (6\text{--}13)$$

where

$$A = \frac{a^2\pi}{4} \tag{6--14}$$

where a = aperture of the transmitting antenna.

6.2.3 Transmitter Loss

Transmitter loss is a measured loss that is caused by aberrations due to imperfection in the manufacturing process and mechanical stresses on the optics result in a non-perfect optical wavefront. Each optical surface that the ray traverses causes an optical loss that is multiplicative. This multiplicative loss causes a degradation of the transmit power. In our analysis, this loss is considered to be negligible.

6.2.4 Free Space loss

The free space loss is given by

$$L_R = \frac{\lambda}{4\pi R^2} \tag{6--15}$$

where R = Distance over which the link has to be established.

6.2.5 Receiver gain

The gain of the receiving antenna is given by

$$G_r = (4\pi A)/\lambda \tag{6--16}$$

where

$$A = (a^2\pi)/4 \tag{6--17}$$

where a = aperture of receiving antenna.

6.2.6 Receiver Loss

The loss at the receiver is similar to the loss that occurs at the transmitter but arises from the optical elements at the receiving terminal.In our analysis, this loss is considered to be negligible.

6.2.7 Optical Link Budget Parameters

The parameters for simulation of the optical system are detailed in 6-4 and the transmitted laser signal shown in figure 4-3.The parameters of importance include the gain of the transmitting antenna, power of the transmiting antenna, laser diode drive current, wavelength of operation, range loss, loss at the transmitter, data rate, gain of the receiver and bit error rate.

Table 6-4. Cubesat optical link parameters

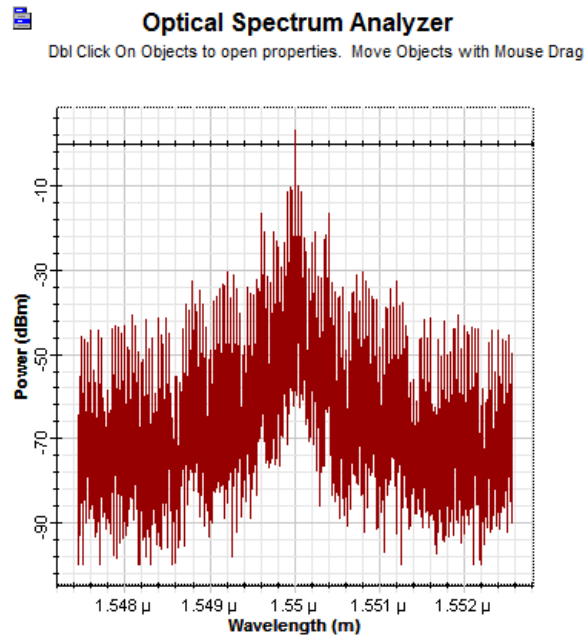| Parameter	Value
G_t	10.36(dB)
P_t	-20(dBW)
Laser Diode Drive Current	10-20(mA)
λ	1550(nm)
L_R	Variable
L_t	0(dB)
Data Rate	120(Mbps)
G_r	10.36(dB)
Bit Error Rate	0

Figure 6-2. Transmitted laser signal

6.2.8 Radio Frequency Link Budget Parameters

The radio frequency link budget parameters are tabulated in 6-5 from [24] for comparison. These experimental parameters are chosen due the frequency of operation being not as far away from the terahertz range when compared to the existing frequency specifications of 430MHz for the CubeSat. The link distances are calculated using the standard RF link budget equations .

Table 6-5. Cubesat radio frequency parameters

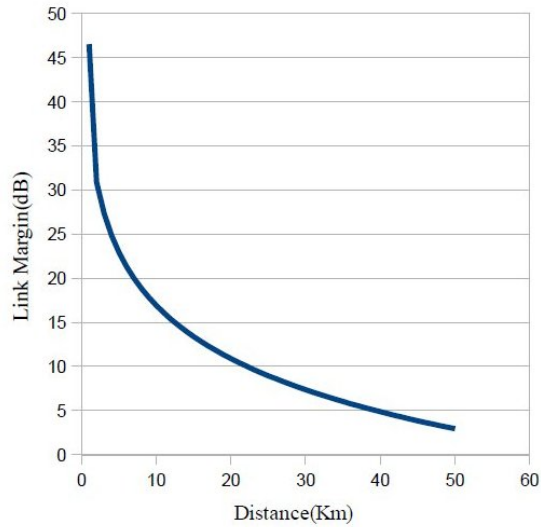| Parameter	Value
EIRP	-21.9(dBW)
G_t	10.36(dB)
P_t	-32.26(dBW)
Frequency	$5.85 * 10^9$(Hz)
L_R	
Polarization Loss	-0.3(dB)
System Noise	135(Kelvin)
Data Rate	1200(bps)
G_r	10.36
E_b/N_o	9.6(dB)
Bit Error Rate	10^{-5}

6.3 Results

Figure 6-3. Intersatellite communication distance with RF links
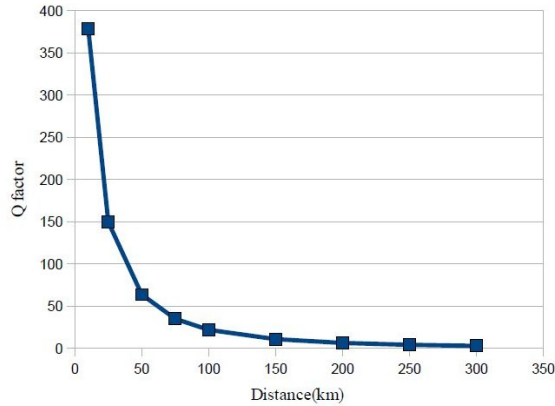
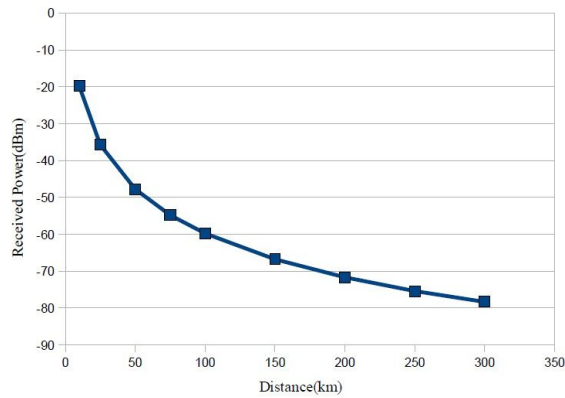Figure 6-4. Q factor of the optical link vs link distance

Figure 6-5. Received power vs link distance

In figure 6-3 the link margin vs. the inter satellite link distance are plotted. The figure shows as the distance between the satellites increases the link margin to achieve a bit error rate of 1E-6 decreases. Since a signal to noise ratio of 3dB has to be maintained to ensure that the BER does not drop below the specified value, the maximum achievable distance for the specified parameters is 50km.

In figure 6-4 the Q factor vs. the inter satellite link distance and in figure 6-5 the received signal power vs. inter satellite link distance is plotted. The Q factor is a measure of the signal to noise ratio of a binary optical signal. For Q factor values greater than 10 and distances less than 200km, the BER is almost 0 thus meeting specifications.This result is further substantiated by the figure 6-6 which show the
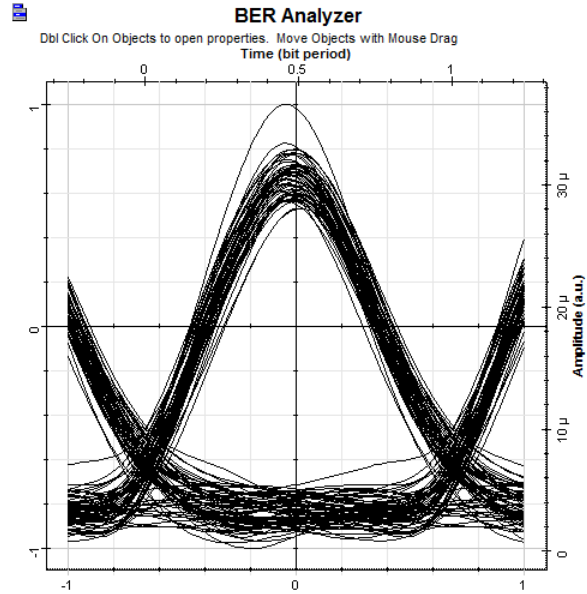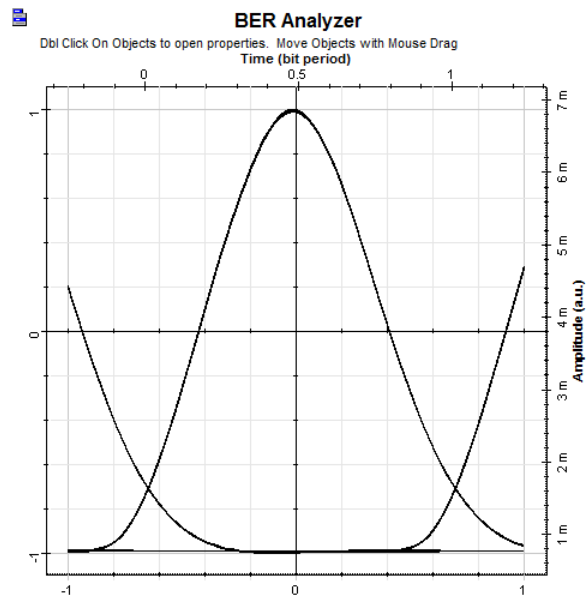
61

Figure 6-6. BER at 150km

Figure 6-7. BER at 10Km

Bit Error Rate Pattern at the receiver. The less erroneous the signal the wider the eye opening. As the signal becomes erroneous the eye height reduces and when the signal is degraded to such an extent as to be unrecognizable at the receiver end, the eye height becomes zero. But for distances greater than 200km where the Q factor

is less than 6 and hence the BER can vary from 1E-9 to 1E-2. As can be observed for distances greater than 200km, the height of the eye is reduced indicating that the probability of detecting the signal correctly has reduced. For distances greater than 250km, the eye height become zero and the signal cannot be detected at all.The scenario considered here is a highly optimistic scenario as the BER for the simulated system is set at 0. Through the results obtained we have thus quantified the maximum achievable inter satellite optical links distances for small satellites for the parameters listed in 6-5

CHAPTER 7
CONCLUSIONS

The thesis has explored the components of an Intersatellite Laser Link System for large satellites that is responsible for establishing cross links as a means of communication and the feasibility of a similar system to achieve long distance crosslinks for the CubeSat. A brief study of the laser crosslink system of the large satellites was provided. Then, the parameters and requirements of the subsystems were discussed and determined for the CubeSat frame. An analysis of the contribution to the weight of the CubeSat and power consumption requirements are performed with respect to the CubeSat specifications. The final parameters were then plugged into a communication system and corresponding link budget analysis and comparision with the RF system were carried out through simulations. We saw that the optical system did not meet the power requirements of the CubeSat but satisfied the weight and volume constraints of the CubeSat. The maximum crosslink range for the CubeSat was determined to be 200km with a BER of 1E-9 to 1E-2 at a date rate of 1Gbps when compared to the Radio Frequency system whose maximum intersatellite distance was determined to be 50km at a data rate of 12kbps. For future work, investigation of an compact Optical System for small satellites whose wet masses are $> 3kg$ and less than 10kg can be carried out.

ABERRATIONS

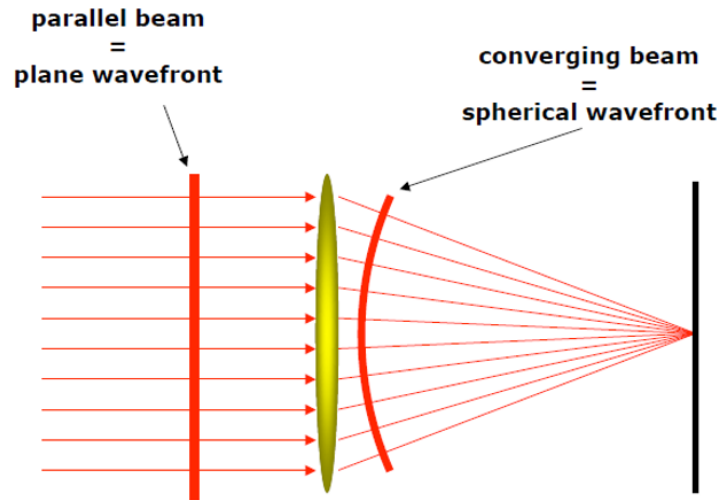A clear representation of aberrations can be explained by inspecting the figures A-1, A-2, A-3, A-4.
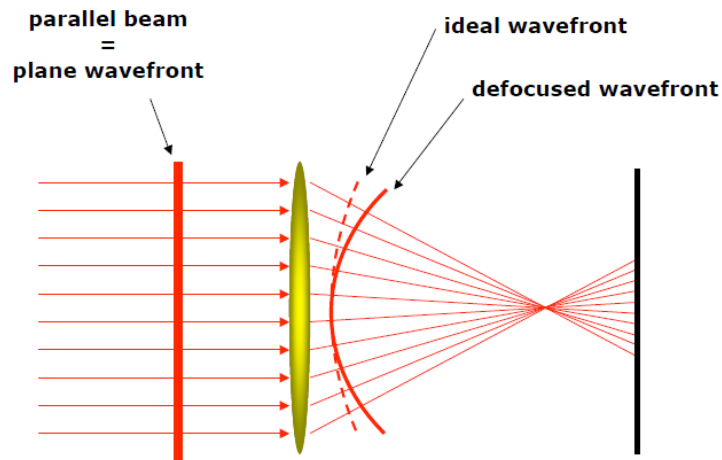

Figure A-1. Without aberration

Figure A-2. Aberration

ASTIGMATISM

Diode lasers are p-n junction devices, where radiation created by injection of carriers across the junction is confined by a tiny optical waveguide. This waveguide,
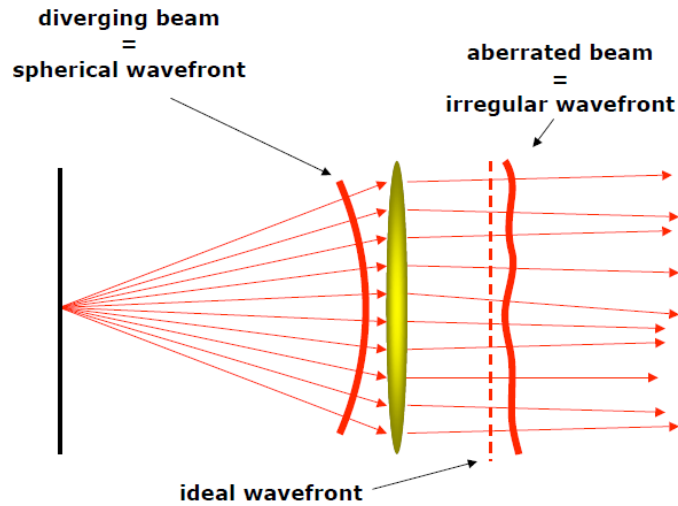
Figure A-3. Aberration
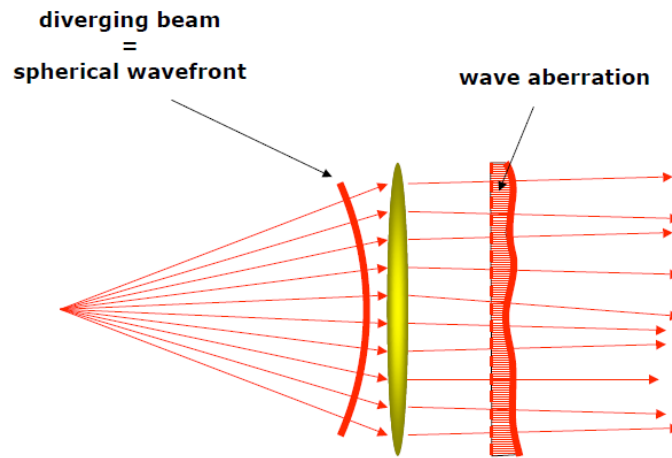
Figure A-4. Aberration

with its plano, partially reflecting end facets perpendicular to the junction, forms the Fabry-Perot cavity of the diode laser. Two general types of optical waveguides may be found in diode lasers. The first is a dielectric slab, or index-guided, waveguide, in which the optical energy is confined through total internal reflection. This is achieved by surrounding the gain region with layers of material with a lower refractive index. In a gain-guided optical waveguide, in contrast, the energy is confined by surrounding the optical gain region with a region of optical loss. It is the guiding mechanism of the

Figure A-5. Astigmatism

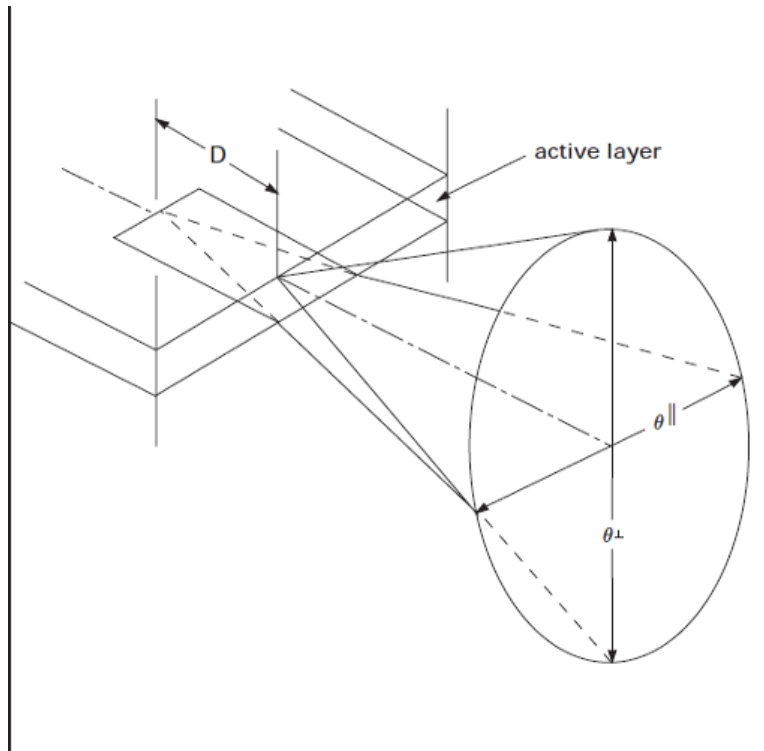waveguide that determines how much astigmatism will be present at the output facet of a diode laser.In index-guided diode lasers, index-guiding is the principal guiding mechanism both parallel and perpendicular to the junction plane. In these lasers, the phase front of the optical wave is planar in both directions, and the wavefront emitted from the laser will have its waists, both perpendicular and parallel to the junction, located at the output facet of the waveguide. In gain-guided diode lasers, gain-guiding is the guiding mechanism in the junction plane and index-guiding is the guiding mechanism perpendicular to the junction plane. In this type of laser. the wavefront exiting from the diode laser is cylindrical. The beam waist perpendicular to the junction plane is still located at the output facet of the diode laser, but the waist parallel to the junction plane is displaced a distance, D, behind the facet . This distance is the longitudinal astigmatism inherent in the diode laser and must be considered when designing optical systems incorporating these lasers.Astigmatism can be represented as shown in A-5.

BEAM RADIUS

The beam radius w is the distance from the beam axis where the optical intensity drops to $1/e^2$ (13.5%) of the value on the beam axis. At this radius, the electric field strength drops to $1/e$ (37%) of the maximum value.For arbitrary (possibly not Gaussian) beam shapes, several different definitions are common. It is possible to still use the $1/e^2$ intensity criterion, or a full width at half-maximum (FWHM), or a radius including 86% of the beam energy, etc. The problem with this type of definitions is essentially that the result does not depend on, e.g., how quickly the intensity decays in the wings of the profile. To illustrate this, 6-3 shows two intensity profiles which have the same FWHM width, although the dashed curve is clearly wider in a meaningful sense. In the case of complicated intensity patterns, it is even more obvious that an FWHM definition cannot be appropriate. For such reasons (and another reason, which is discussed below), the recommended definition is that of ISO Standard 11146, based on the second moment of the intensity distribution I(x,y).

$$w_x = 2 * \frac{\sqrt{\int x^2 * I(x,y)\mathrm{d}x\mathrm{d}y}}{\int I(x,y)\mathrm{d}x\mathrm{d}y} \tag{A–1}$$

For example, the beam radius in the x direction is where the coordinates x and y must be taken to be relative to the beam center, i.e., such that the first moments vanish.

BEAM DIVERGENCE

The beam divergence of a laser beam is a measure of how fast the beam expands far from the beam waist,i.e in the so called far field. A low beam divergence is important for applications such as free space communications and. Beams with an approximately constant beam radius over significant propagation distances are called collimated beams. A-7 visually represents the beam divergence that effects lasers.

NUMERICAL APERTURE

The numerical aperture of an optical system is a dimensionless parameter that characterizes the range of angles that the system can accept or emit light. The f number
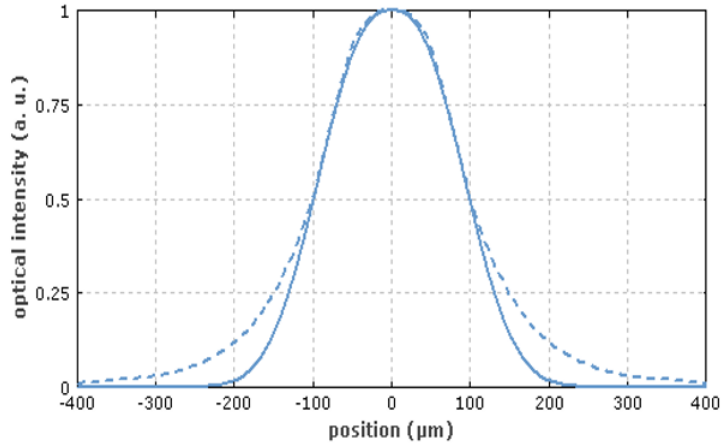
Figure A-6. Beam radius
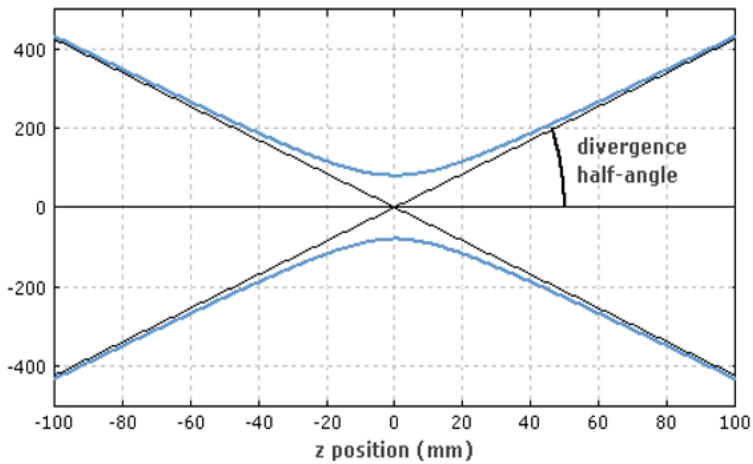
Figure A-7. Beam divergence

of a lens shown in figure is given by $N = f/D$ where f is the focal length of the lens and D is the diameter of the entrance pupil. The numerical aperture(NA) is given by:

$$NA = n * sin(\theta) = n * sin(\arctan(D \div 2f))$$ (A–2)

assuming n=1 for air.The approximation holds when the numerical aperture is small, and it is nearly exact even at large numerical apertures for well-corrected camera lenses. For numerical apertures less than about 0.5 (f-numbers greater than about 1) the divergence between the approximation and the full expression is less than 10%. Beyond this,

the approximation breaks down. The numerical aperture for a laser is defined slightly differently. Laser beams spread out very slowly as they propagate. Far away from the narrowest part,the spread is roughly linear with distance-the laser beam forms a cone of light in the far field. The numerical aperture is given by

$$N = n * sin(\theta) \tag{A–3}$$

where θ is the angle of divergence in the far field pattern. For a Gaussian beam profile described previously,the NA is related to its minimum spot size by

$$NA \approx \frac{2\lambda}{\pi D} \tag{A–4}$$

where is λ is the wavelength of light in vacuum and D is the diameter of the beam in the narrowest spot. A-8 shows the numerical aperture of a lens.

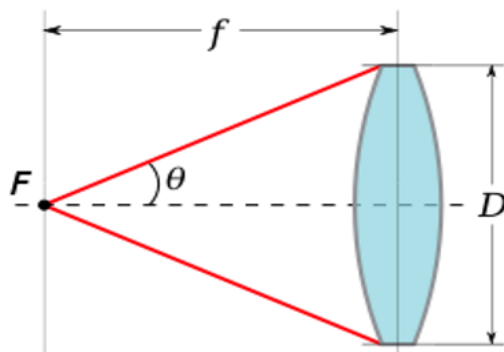Figure A-8. Numerical aperture

POINT AHEAD ANGLE

One critical aspect of inter satellite laser communications with narrow beams results from the need to introduce a point ahead angle. Due to the finite velocity of light and relative angular velocity of two communication terminals moving in space, the transmit beam must be directed towards the receiver's position it will have some later time. This
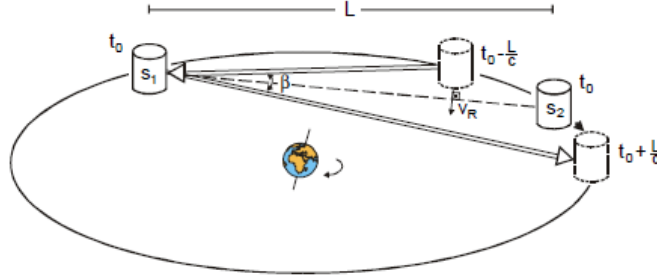
Figure A-9. Point ahead angle

point ahead angle is given by:

$$\beta = \frac{v_r}{c} \qquad \text{(A–5)}$$

where β is the point ahead angle and v_r is the relative velocity component orthogonal to the line of sight of the satellite and c is the velocity of light. Point ahead angle is generally 40microrad for GEO-GEO link and 70microrad for LEO-GEO link. The point ahead angle is generally greater than the beam width. It can be introduced either in the receive or transmit path and must be varied as varies with time. Since it is difficult to design a control loop for automatic point ahead adjustment,todays concepts rely on calculation of point ahead angles based on known ephemeris data. The point ahead assembly hence is used to direct the transmit or receive beam accordingly. A-9 represents the point ahead angle.

RAYLEIGH WAVELENGTH

The Rayleigh length (or Rayleigh range) of a laser beam is the distance from the beam waist (in the propagation direction) where the beam radius is increased by a factor of the square root of 2. For a circular beam, this means that the mode area is doubled at this point. For Gaussian beams, the Rayleigh length is determined by the waist radius w_o and the wavelength λ:

$$z_r = \pi * w_c^2 / \lambda \qquad \text{(A–6)}$$

where the wavelength λ is the vacuum wavelength divided by the refractive index n of the material and is the Rayleigh length.

WAVEFRONT ERROR

The extent of image deterioration caused by wavefront deformations is determined by its deviation from spherical, averaged over the entire wavefront. It is the so called root-mean-square (RMS) wavefront error, usually expressed in units of the wavelength of light. It is a square root of the difference between the average of squared wavefront deviations minus the square of average wavefront deviation, or RMS=, with the brackets indicating average value. For instance, if we measure wavefront deviations at three points (for simplicity) as 0.5, 0.2 and 0.1, the average of their squared values W2=0.1, while the square of their average value W2=0.071. The RMS error would be given as RMS==0.17. This amounts to a standard, or statistical deviation from a perfect reference sphere over the entire wavefront. To be meaningful, the RMS wavefront error has to be calculated for a large number of points on the wavefront (or optical surface, for the surface RMS).

REFERENCES

[1] G. Stephen and L. William, *Laser Communications in Space.* Massachusetts: Artech House, 1995.

[2] G. Willebrand, *Free Space Optics: Enabling Optical Connectivity in Today's Networks*. Indiana: Sams Publishing, 2001.

[3] A. Kenichi, I. Keizo, and Y. Koji, "Design of a compact transceiver optical system for optical inter satellite links." *Proceedings of SPIE*, vol. 1218, pp. 169–177, 1990.

[4] D. Vukobratovich, "Ultra-lightweight optics for laser communications," *Free-Space Laser Communication Technologies II*, vol. 1218, pp. 501–505, 1990.

[5] Z. Sodnik, B. Furch, and H. Lutz, "Free-space laser communication activities in europe: Silex and beyond," *IEEE LEOS Annual Meeting Conference Proceedings*, vol. 1, pp. 78–79, 2006.

[6] J. K. Herbert and P. C. Arthur, "An overview of small satellites in remote sensing," *International Journal of Remote Sensing*, vol. 15, pp. 4285 – 4337.

[7] R. Munataka, "Cubesat design specifications," California Polytechnic State University, Tech.Report, 2009.

[8] A. Siegman, *Laser*. California: University Science Books, 1986.

[9] J. Mulholland and S. Cadogan, "Intersatellite laser crosslinks," *IEEE Transactions on Aerospace and Electronic Systems*, vol. 32, 1996.

[10] R. G. Marshalek and D. K. Paul, "Mass, prime power and volume estimates for reliable optical intersatellite link payloads," *Free-Space Laser Communication Technologies II*, vol. 1218, pp. 40–50, 1990.

[11] R. L. Walter, K. Andras, H. K. Klaus, J. W. Peter, and F. Bernhard, "Optical cross-links for microsatellite fleets," *20th AIAA International Communication Satellite Systems Conference*, no. AIAA 2002-2003, 2002.

[12] P. C. Hobbs., *Building electro-optical systems : optics that work*. Wiley.

[13] M. Bailly, "Pointing, acquisition, and tracking system of the european silex program: a major technological step for intersatellite optical communication," *Proceedings of SPIE*, vol. 1417, pp. 142–157, 1991.

[14] M. F. Hueber and A. L. Scholtz, "Heterodyne acquisition and tracking in a free-space diode laser link," *Proceedings of SPIE*, vol. 141, pp. 233–239, 1991.

[15] P. Bandera, "A fine pointing mechanism for intersatellite laser communications," *Proceedings of the 8th European Symposium*, vol. 38, 1999.

[16] P. Adoph, W. Coppoolsea, and J. Moerschellb, "Development and test of a fine pointing assembly for optical satellite communications," *Proceedings of SPIE*, vol. 4902, pp. 679–690, 2002.

[17] D. Buvat, G. Muller, and P. Peyrot, "The coarse pointing assembly for silex program or how to achieve outstanding pointing accuracy with simple hardware associated with consistent control laws." *Free Space Laser Communciation Technologies III*, vol. 1417, pp. 251–261, 1991.

[18] R. T. Carlson, "Technologies and techniques for lasercom terminal size, weight, and cost reduction," *Free-Space Laser Communication Technologies II*, vol. 12, pp. 62–69, 1990.

[19] R. A. Cockshott and P. J. David, "Silex acquisition and tracking sensors," *Free-Space Laser Communication Technologies VII*, vol. 2381, pp. 206–214, 1995.

[20] K. Shiratama, "Fine pointing mechanism using multi-layered piezo-electric actuator for optical isl system," *Proceedings of SPIE*, vol. 1218, pp. 117–128, 1990.

[21] D. Scroeder, *Astronomical Optics*.   San Diego, CA: Academic Press, 1987.

[22] C. F. JR and a. et, "Simulink blocks for simulation of light sources," *Microwave and Optoelectronics Conference*, vol. 2, pp. 501–505, 1999.

[23] H. A. Ghezal and A. Ouchar, "Design and conception of optical links simulator for telecommunications applications under simulink environmen," *5th WSEAS Intl. Conference on Applied Electromagnetics, Wireless and Optical Communications*, 2007.

[24] S. Timoty, T. Aaron, and A. T. Michael, "Active antennas for cubesat applciations," *Small Satellite Conference*, vol. SSC02-V-2, 2002.

[25] K. Birnbaum, W. Farr, J. Gin, B. Moision, K. Quirk, and M. Wright, "Demonstration of a high-efficiency free-space optical communications link," *Proceedings of SPIE*, 2009.

[26] D. M. Boroson, "Lite engineering model-i: operation and performance of the communications and beam-control subsystems," *Free-Space Laser Communication Technologies V*, vol. 1866, pp. 73–82, 1993.

[27] F. Capasso, R. Paiella, R. Martini, R. Colombelli, C. Gmachl, T. Myers, M. Taubman, R. Williams, C. Bethea, K. Unterrainer, H. Hwang, D. Sivco, a.Y. Cho, a.M. Sergent, H. Liu, and E. Whittaker, "Quantum cascade lasers: ultrahigh-speed operation, optical wireless communication, narrow linewidth, and far-infrared emission," *IEEE Journal of Quantum Electronics*, vol. 38, no. 6, pp. 511–532, 2002.

[28] W. L. Casey, "Design considerations for air-to-air laser communications," *Free-Space Laser Communication Technologies III*, vol. 1417, pp. 89–98, 1991.

[29] B. J. Cassarly, J. C. Ehlert, and D. J. Henry, "Low insertion loss high precision liquid crystal optical phased array bill," *Free-Space Laser Communication Technologies III*, vol. 1111, pp. 110–121, 1991.

[30] Y. Koji, G. Koji, K. Kanshiro, and A. Kenichi, "Configuration and performance of optical modulator demodulator for optical intersatellite communications," *Free-Space Laser Communication Technologies II*, vol. 1218, pp. 348–354, 1990.

[31] F. M. Davidson, "Bandwidth requirements for direct detection optical communication receivers with ppm signaling," *Proceedings of SPIE*, vol. 1417, pp. 75–88, 1991.

[32] A. Cosson, P. Doubrere, and E. Perez, "Simulation model and on-ground performances validation of the pat system for silex program the pointing acquisition and tracking (pat) subsystem of the european silex program," *Free-Space Laser Communication Technologies-III*, vol. 1417, pp. 262–276, 1991.

[33] P. Discussion, "Rf vs laser communications (transcript)," *Free-Space Laser Communication Technologies V*, vol. 1866, pp. 304–340, 1993.

[34] A. Dommann, "Fine pointing device for intersatellite link," European Space Components Information Exchange System, Tech.Report, 2010.

[35] D. Driemeyer, A. Chenoweth, D. Dreisewerd, S. Lambert, T. Morris, M. Douglas, and A. W. Louis, *Free-Space Laser Communication Technologies V*.

[36] O. Duchmann, "How to meet intersatellite links mission requirements by an adequate optical terminal design," *Proceedings of SPIE*, vol. 1417, pp. 30–41, 1991.

[37] R. Dumas, "System test bed for demonstration of the optical space communications feasibility," *Proceedings of SPIE*, vol. 1218, pp. 398–411, 1990.

[38] A. Gardam, "Stability considerations in relay lens design for optical communications," *Free-Space Laser Communication Technologies III*, vol. 1417, pp. 381–390, 1991.

[39] F. Herzog, K. Kudielka, D. Erni, and W. Bächtold, "Optical phase locked loop for transparent inter-satellite communications." *Optics express*, vol. 13, no. 10, pp. 3816–21, 2005.

[40] U. Hildebrand, "A high performance laser diode transmitter for optical free space communications," *Free Space Laser Communications Technologies II*, vol. 1218, pp. 216–227, 1990.

[41] K. Inagaki, M. Nohara, K. Arakit, M. Fujise, and Y. Furuhama, "Free space simulator for laser transmitter," *Free-Space Laser Communication Technologies-III*, vol. 1417, pp. 160–169, 1991.

[42] Imaging properties of lens systems. [Online]. Available: www.mellesgriot.com

[43] J. E. Kaufmann and E. A. Bucher, "Free-space optical code-division multiple-access system design," *Free-Space Laser Communication Technologies V*, vol. 1866, pp. 167–179, 1993.

[44] I. KVICALA, "Temperature dependency of semiconductor," Brno University of Technology, Tech. Rep., 2005.

[45] W. R. Leeb, "Space laser communications : Systems, technologies and applications," Institution of Communication and Radio-Frequency Engineering, Viena University of Technology, Tech.Report, 1998.

[46] S. P. Levitan, T. P. Kurzweg, J. A. Martinez, D. M. Chiarulli, and P. J. Marchand, "Simulations for free space interconnects," *Optical Society of America*, pp. 5–7.

[47] R. Ludwig, M. Galili, B. Huettl, F. Futami, S. Watanabe, and C. Schubert, "160 gbit / s all-optical ook to dpsk in-line format conversion," Fraunhofer Institute for Telecommunications, Heinrich-Hertz-Institut, Tech.Report, 2006.

[48] G. S. Mecherle, R. J. Henderson, and R. Beach, "Comparison of simulation and experimental measurements of avalanche photodiode receiver performance," *Free-Space Laser Communication Technologies III*, vol. 1417, pp. 537–542, 1991.

[49] G. S. Mecherle and D. Smith, "Next-generation 3-gbps coherent optical space communication terminal under 100 lbs, 100w," *Free-Space Laser Communication Technologies V*, vol. 1866, pp. 158–166, 1993.

[50] G. S. Mecherle, "Trw laser communication simulations," *Free-Space Laser Communication Technologies I*, vol. 1218, pp. 597–608, 1990.

[51] B. Menke and R. Lffler, "Comparative life test of o.8um -laserdiodes for silex under nrz and qppm modulation," *Free-Space Laser Communication Technologies III*, vol. 1417, pp. 316–327, 1991.

[52] T. N. Toni, "Pointing, acquisition and tracking system for the free space laser communication system silex," *Free-Space Laser Communication Technologies VII*, vol. 2381, pp. 194–205, 1995.

[53] R. A. Peters, "Intersatellite links," *International Journal of Satellite Communications*, vol. 6, no. 2, pp. 79–80, 1988.

[54] D. Robinson, C.-C. Chen, and H. Hemmati, "An electro-optic resonant modulator for coherent optical communication," *Free-Space Laser Communication Technologies III*, vol. 1417, pp. 421–430, 1991.

[55] A. Roorda, "Optics , wavefront and geometrical optics relationships between pupil size , refractive error and blur," University of California, Berkeley, Tech.Report.

[56] R. C. Short, "Acquisition and tracking performance measurements for a high-speed area array detector system," *Proceedings of SPIE*, vol. 1417, pp. 131–141, 1991.

[57] I. S. Reed and G. Solomon, "Polynomial codes over certain finite fields,," *SIAM Journal of Applied Math*, vol. 8, pp. 300–304, 1960.

[58] R. J. Smith, "Resonant laser receiver for free-space laser communications," *Proceedings of SPIE*, vol. 1635, pp. 19–26, 1992.

[59] X. Sun, F. Davidson, and C. Field, "50 mbps free space direct detection laser diode optical communication system with q=4 ppm signaling," *Free-Space Laser Communication Technologies I*, vol. 1218, pp. 385–395, 1990.

[60] C. Tan and R. T. Carison, "Liquid crystals for lasercom applications," *Free-Space Laser Communication Technologies III*, vol. 1417, pp. 391–401, 1991.

[61] D. Vukobratovich, "Ultra-lightweight optics for laser communications," *Free-Space Laser Communication Technologies II*, vol. 1218, pp. 178–192, 1990.

[62] K. E. Wilson, "Prediction of the required received optical power for bipolar raised cosine modulation," *Free-Space Laser Communication Technologies I*, vol. 1218, pp. 355–373, 1990.

[63] J. C. Wyant and K. Creath, *Basic Wavefront Aberration Theory for Optical Metrology*. New York: Academic Press Inc., 1992.

BIOGRAPHICAL SKETCH

Seshupriya Alluru received her master's degree from the Department of Electrical and Computer Engineering in the fall of 2010. She has a bachelor's degree from Jawaharlal Nehru Technological University, India in electronics and communications engineering.

As a graduate student, she worked in the wireless and mobile systems laboratory and conducted research on small satellites and wireless sensor networks. Her other research interests include applications of game theory and optimization in wireless communication systems.